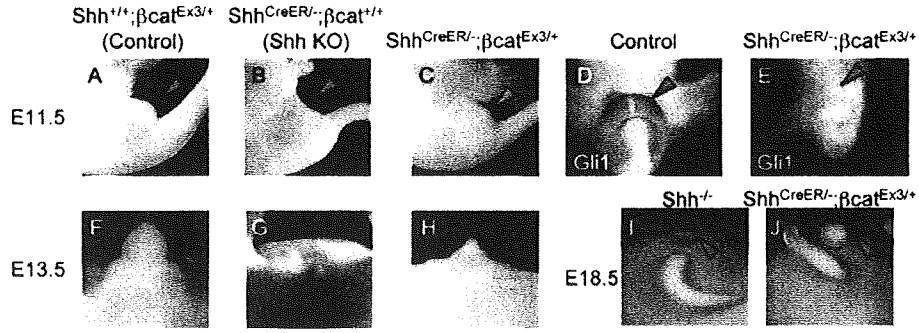

Fig. 6. Rescue of GT outgrowth in *Shh*-null mutants by constitutively active β-catenin. (**A-J**) Control GTs (A,F) and *Shh* KO mouse embryos with GT agenesis (B,G,I). $Shh^{CreERT2/-};Ctnnb1^{Ex3/+}$ embryos have GT protrusion at E11.5 and continued GT outgrowth with preputial fold at E13.5 (C,H). Further outgrowth is evident by E18.5 (J). *Gli1* expression is undetectable in $Shh^{CreERT2/-};Ctnnb1^{Ex3/+}$ embryos at E11.5 (D,E). Arrowheads indicate GT or prospective GT regions.

Integrated Gli and Shh signaling for GT development; hedgehog functions as a trigger for GT initiation and promotes subsequent outgrowth

Several reports have demonstrated the contribution of multiple growth factors to GT development, including hedgehog, Wnt and Fgf signaling (Haraguchi et al., 2001; Haraguchi et al., 2000; Lin et al., 2008; Morgan et al., 2003; Perriton et al., 2002; Suzuki et al., 2003; Yamaguchi et al., 1999). Shh plays a crucial role in external genitalia development (Haraguchi et al., 2001; Perriton et al., 2002). Here, stage-specific *Shh* conditional mutant analysis reveals the temporal requirements for *Shh* function during GT development. Early loss of *Shh* function induces minimal GT outgrowth and the cloaca persists, but later gene ablation elicits milder GT phenotypes. This might recapitulate early, transient requirements for *Shh* for the rapid growth of digit primordia (and digit patterning) in the limb (Zhu et al., 2008), and epithelium-derived *Shh* function in regulating tooth organ size (Dassule et al., 2000). Several pathways have been postulated to regulate proximal-distal and dorsal-ventral axis formation of the GT (Suzuki et al., 2003; Suzuki et al., 2008; Yamada et al., 2003; Yamada et al., 2006). If Shh only functions as a growth-promoting factor during early GT development, axis marker gene expression should have been normal in the early *Shh* conditional mutant GTs. However, *Dlx5* and *Wnt5a* expression was abnormal, suggesting that proximal-distal axis formation was altered by early loss of *Shh* function. However, it is necessary to consider the unique character of GT development, as its robust outgrowth from the beginning depends substantially on *Shh*. Namely, the proximal-distal patterning is tightly linked with such robust outgrowth promotion of the anlage. Hence, it is not simply possible to make a conclusion for the status of proximal-distal axis formation by the current data. By contrast, expression of *Pitx1*, as a candidate dorsal marker during GT development (our unpublished results) (Haraguchi et al., 2007), was unaffected by loss of Shh function. It has recently been suggested from lineage analysis that the dorsal side of the GT develops in association with more-anterior regions, including the peri-cloacal mesenchyme (PCM) and the lower body wall regions (Haraguchi et al., 2007). The sustained dorsal marker gene expression might reflect such a unique program of GT development and the nature as a dorsal structure is less affected by *Shh*.

Hedgehog signal transduction comprises a series of complex intracellular events. Shh signaling modulates the function of Gli transcription factors. In mammals, Gli2 is a major positive transcriptional effector of hedgehog signal transduction. In the absence of Shh, Gli2 is completely degraded, and Gli3 is converted into a transcriptional repressor, Gli3R (Ingham and McMahon, 2001). By titrating the relative amounts of these factors, we found that both the extent of GT outgrowth and the level of Wnt/β-catenin activity are responsive to the effective level of hedgehog signaling. In the wild-type situation, Shh activates Wnt/β-catenin signaling and GT outgrowth, but in *Shh* KO embryos the net effect of the absence of Gli2 activator and presence of Gli3R leads to the most severe phenotype: GT agenesis. The contribution of Gli3R to the *Shh* KO phenotype is indicated by the restoration of TopGAL activity and moderate GT outgrowth in *Shh;Gli3* double mutants ($Shh^{-/-};Gli3^{xt/xt}$). Shh activity during GT outgrowth is likely to prevent formation of Gli3R. In *Gli2* KO embryos, Shh prevents formation of Gli3R, but loss of Gli2 activator causes a modest decrease in downstream Wnt/β-catenin activity and the phenotypic outcome is GT hypoplasia. Thus, normal GT development requires the Shh pathway as balanced by the activation of Gli2 and Gli3. Integrated Gli function has been thoroughly explored with regard to anterior-posterior patterning of the limb, in which a major role of Shh is to prevent formation of Gli3R (Nieuwenhuis and Hui, 2005). In the GT, Gli2 activation downstream of Shh is essential for outgrowth, and inhibition of Gli3R production appears less important.

Context-dependent cross-talk between Wnt/β-catenin and Shh signaling

Shh KO embryos exhibit failed GT outgrowth and loss of *Fgf8* expression in the DUE (Haraguchi et al., 2001; Perriton et al., 2002). In addition to our finding that hedgehog signaling regulates the level of Wnt/β-catenin activity in a dosage-dependent manner, we found that Wnt/β-catenin in turn regulates *Fgf8* expression. Surgical removal of the ectodermal epithelium results in GT truncation, indicating an inductive role of the ectodermal epithelium in GT development (Murakami and Mizuno, 1986). We found that the expression of several ectodermal Wnt ligand genes was reduced in *Shh* KO embryos. Indeed, Wnt/β-catenin activity in the cloacal membrane and later DUE was affected by the level of hedgehog signaling. Ectoderm-derived Wnt ligands are likely candidates for induction of Wnt/β-catenin activity in the distal GT, including the DUE. In the limb, ablation of *Wnt3* from the limb ectoderm results in agenesis as the most severe outcome, suggesting a similarly essential role for ectodermal Wnt ligands in appendicular outgrowth (Barrow et al., 2003).

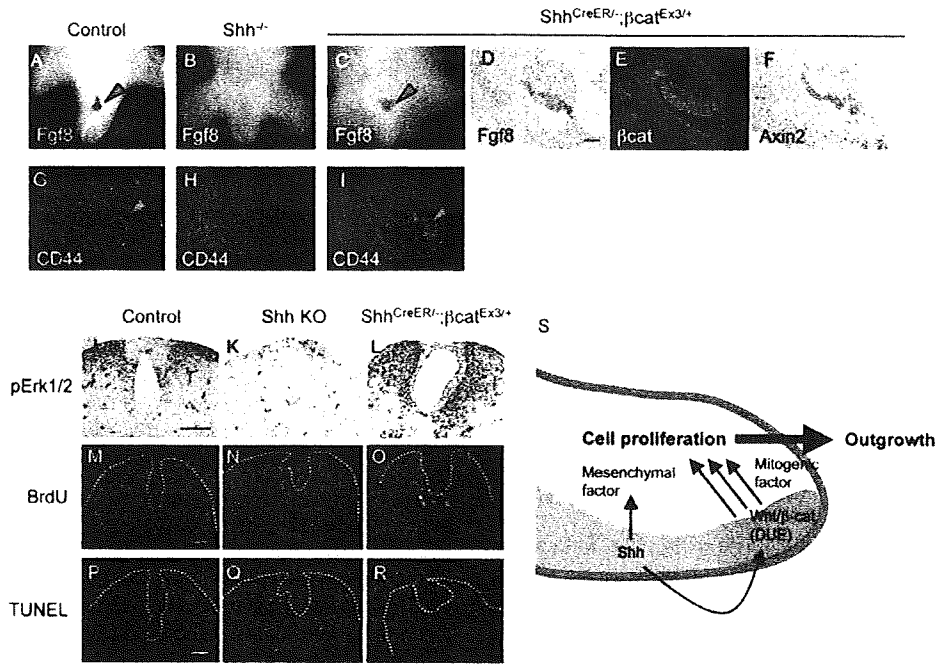

Fig. 7. Regulation of *Fgf8* expression by Shh and β-catenin. (**A-I**) *Fgf8* (A,B) and Cd44 (G,H) expression (arrowheads) in control (A,G) versus *Shh* KO (B,H) DUE. Expression is recovered in $Shh^{CreERT2/-};Ctnnb1^{Ex3/+}$ embryos (arrows in C,I). *Fgf8* and Cd44 expression overlap with regions of augmented β-catenin and *Axin2* (D-F,I). (**J-L**) pErk1/2 staining in control (J) versus *Shh* KO (K) and $Shh^{CreERT2/-};Ctnnb1^{Ex3/+}$ (L) embryos. (**M-R**) BrdU labeling (M-O) and TUNEL assays (P-R). *Shh* KO embryos show significantly decreased cell proliferation (N). By contrast, expression of stabilized β-catenin in *Shh* KO mutants restores cell proliferation (O). Mesenchymal apoptosis was unchanged in $Shh^{CreERT2/-};Ctnnb1^{Ex3/+}$ embryos as compared with *Shh* KO embryos (Q,R). Dotted lines in the midline GT indicate the basal layer of the endodermal and ectodermal epithelia. (**S**) Proposed signaling cascade for GT outgrowth. Shh signaling is required for GT initiation and subsequent outgrowth. *Shh* is expressed moderately in the DUE (red) and strongly in urethral epithelium (orange). Wnt ligands are expressed in the distal GT ectoderm, and Wnt/β-catenin activity is detected in the distal region of the GT, including the DUE. Wnt/β-catenin activity depends on Shh signaling. This Wnt/β-catenin activity, and possibly urethral plate-derived Shh, induce production of mitogenic factors leading to GT outgrowth. Yellow, mesenchyme; blue line, ectoderm-derived epithelium. Scale bars: 100 μm.

Given the strong Wnt/β-catenin activity in the endoderm-derived DUE, we used temporally inducible $Shh^{CreERT2}$ to analyze the effects of β-catenin loss-of function in the endoderm during GT outgrowth. $Shh^{CreERT2};Ctnnb1^{lox}$ embryos treated with TM at E9.5 exhibited markedly reduced *Fgf8* expression. However, *Gli1* expression was normal at E11.5, indicating that Shh signaling was not affected by disrupting Wnt/β-catenin signaling at this later stage. Taken together with the results of our β-catenin gain-of-function studies (see below), Wnt/β-catenin signaling appears to be downstream of hedgehog signaling during GT outgrowth and upstream of *Fgf8* expression.

Wnt/β-catenin signaling is required during early embryogenesis (E9.0) for the formation of the caudal embryo and $Wnt3a^{-/-}$, $Lef1^{-/-};Tcf1^{-/-}$ and $Tcf1^{-/-};Tcf4^{-/-}$ embryos exhibit severe caudal truncation of the embryonic axis and GT agenesis (Dunty et al., 2008; Galceran et al., 1999; Gregorieff et al., 2004; Takada et al., 1994). Owing to the wide range of Wnt/β-catenin functions, the epistatic relationships between hedgehog and Wnt/β-catenin signaling are likely to vary in different developmental contexts. To investigate such a possibility with regard to GT development, we conditionally ablated β-catenin with $Isl1^{Cre}$, in which Cre is active in the prospective GT region at the stage required for caudal body formation (~E9.0). $Isl1^{Cre/+};Ctnnb1^{lox/lox}$ embryos exhibited a loss of *Shh* expression at this early stage, consistent with the proposal that *Shh* lies downstream of β-catenin in the endoderm (Lin et al., 2008). The importance of Wnt/β-catenin activity during formation of the caudal embryo suggests that Wnt/β-catenin activity might contribute to cloaca formation, a possibility that merits further study.

Possible regulation of *Fgf8* expression by β-catenin and functional redundancy among Fgfs during GT outgrowth

The CR3 enhancer (located 24 kb 3′ of the *Fgf8* coding region) contributes to *Fgf8* expression in the AER (Beermann et al., 2006). *Fgf8* expression is augmented in the limb by overexpression of stabilized β-catenin in the ectoderm (Soshnikova et al., 2003). We questioned whether similar regulatory actions of β-catenin on *Fgf8* expression operate in the DUE via CR3. We found that β-catenin is bound to a region of CR3 in nuclear extracts from GTs and that this region confers a transcriptional response to exogenous β-catenin in luciferase assays. *Fgf8* expression is decreased in both GT and limb bud in β-catenin loss-of-function mutants (this study) (Lin et al., 2008; Soshnikova et al., 2003). These results suggest β-catenin as a candidate upstream regulator of *Fgf8* expression in the DUE. Regulation of *Fgf8* by β-catenin might be a shared characteristic of the AER and DUE. Such regulation through another candidate enhancer in intron 3 of *Fgf8* was recently reported for tooth development (Wang et al., 2009).

Although we found that *Fgf4/8* are largely dispensable for GT development, it is likely that compensation by other Fgf ligands occurs, as has been described in the limb, tooth, inner ear and brain (Boulet et al., 2004; Mariani et al., 2008; Moon and Capecchi, 2000). In the current study, a specific Fgf can be (also ectopically) induced upon mutation of another Fgf. Our data suggest that a feedback mechanism operates to maintain the amount of Fgf signaling emanating from the DUE, and that this mechanism can induce expression of Fgf ligand-encoding genes that are otherwise often undetectable. We have made similar observations in the pharyngeal tissues of *Fgf8* mutants (A.M., unpublished) (Moon et al, 2000). The redundancy of Fgf function can also be analyzed in Fgf receptor (Fgfr) conditional mutants. Our preliminary analyses of conditional Fgfr mutants reveal GT defects (our unpublished results), and *Fgfr1*-null mutants have caudal agenesis (Deng et al., 1994; Yamaguchi et al., 1994). Dispensable *Fgf8* function was also recently demonstrated (Seifert et al., 2009).

The development of an embryonic bud structure requires an expansion of mesenchymal tissue during outgrowth (Sun et al., 2002). We found that constitutively active β-catenin in the DUE induced Erk1/2 phosphorylation and cell proliferation in the adjacent GT mesenchyme. This suggests that Wnt/β-catenin stimulates the distal GT, including the DUE, to secrete mitogenic factors required for GT mesenchymal growth (see Fig. S7 in the supplementary material). However, the nature of these factors is still unclear (see discussion of Fgfs above). We have shown that Bmp7 from the DUE has some role in GT outgrowth, suggesting Bmp signaling as an essential growth regulator of the GT (Suzuki et al., 2008). *Bmp4* is induced by *Shh* and our previous data also suggest roles for Bmp signaling in the DUE and distal ectoderm in GT outgrowth (Suzuki et al., 2003).

Our work reveals both conserved and divergent features of the developmental programs that trigger GT and limb bud formation and how they interact to control subsequent outgrowth. Initiation and outgrowth of the GT primordia also critically influence anorectal/urogenital organ development (Hynes and Fraher, 2004), as revealed by the fact that *Shh* KO mutants display not only GT agenesis, but also a persistent cloaca (Mo et al., 2001). *Gli2* and some conditional *Shh* mutant embryos show a severe form of defects for UPE formation in the GT. Overall, an improved understanding of the molecular mechanisms of genital development might shed light on the mechanisms that underlie congenital abnormalities of multiple organ systems, in addition to those affecting the external genitalia and anorectal/urogenital organs.

Acknowledgements

We thank Drs A. Joyner, C. C. Hui, P. Chambon, A. McMahon, W. Birchmeier, G. Martin, M. Lewandoski, T. P. Yamaguchi, B. Hogan, J. Partanen, L. Ma, T. Tsukiyama, Y. Yamaguchi, K. Araki, K. Yamamura, D. Ornitz, N. Nakagata, S. Kume and S. Takada for their invaluable support; Ms S. Miyaji for assistance; and UCSD and Bristol-Myers Squibb for mouse distribution. This study was supported by Grant-in-Aid for Young Scientists B, Grant-in-Aid for Scientific Research B, and for Scientific Research on Priority Areas; by Mechanisms of Sex Differentiation and General Promotion of Cancer Research in Japan; by the global COE program 'Cell Fate Regulation Research and Education Unit'; by a Grant for Child Health and Development, and a Health Sciences Research Grant from the Ministry of Health, Labour and Welfare. This study was also supported by NIH grant (R01ES016597-01A1). The content is solely the responsibility of the authors and does not necessary represent the official views of the NIH. Deposited in PMC for release after 12 months.

Supplementary material

Supplementary material for this article is available at
http://dev.biologists.org/cgi/content/full/136/23/3969/DC1

References

Ahn, K., Mishina, Y., Hanks, M. C., Behringer, R. R. and Crenshaw, E. B., 3rd (2001). BMPR-IA signaling is required for the formation of the apical ectodermal ridge and dorsal-ventral patterning of the limb. *Development* **128**, 4449-4461.

Araki, K., Imaizumi, T., Okuyama, K., Oike, Y. and Yamamura, K. (1997). Efficiency of recombination by Cre transient expression in embryonic stem cells: comparison of various promoters. *J. Biochem.* **122**, 977-982.

Barrow, J. R., Thomas, K. R., Boussadia-Zahui, O., Moore, R., Kemler, R., Capecchi, M. R. and McMahon, A. P. (2003). Ectodermal Wnt3/beta-catenin signaling is required for the establishment and maintenance of the apical ectodermal ridge. *Genes Dev.* **17**, 394-409.

Beermann, F., Kaloulis, K., Hofmann, D., Murisier, F., Bucher, P. and Trumpp, A. (2006). Identification of evolutionarily conserved regulatory elements in the mouse Fgf8 locus. *Genesis* **44**, 1-6.

Benazet, J. D., Bischofberger, M., Tiecke, E., Goncalves, A., Martin, J. F., Zuniga, A., Naef, F. and Zeller, R. (2009). A self-regulatory system of interlinked signaling feedback loops controls mouse limb patterning. *Science* **323**, 1050-1053.

Boulet, A. M., Moon, A. M., Arenkiel, B. R. and Capecchi, M. R. (2004). The roles of Fgf4 and Fgf8 in limb bud initiation and outgrowth. *Dev. Biol.* **273**, 361-372.

Capdevila, J. and Izpisua Belmonte, J. C. (2001). Patterning mechanisms controlling vertebrate limb development. *Annu. Rev. Cell Dev. Biol.* **17**, 87-132.

Chen, Y., Knezevic, V., Ervin, V., Hutson, R., Ward, Y. and Mackem, S. (2004). Direct interaction with Hoxd proteins reverses Gli3-repressor function to promote digit formation downstream of Shh. *Development* **131**, 2339-2347.

Chiang, C., Litingtung, Y., Lee, E., Young, K. E., Corden, J. L., Westphal, H. and Beachy, P. A. (1996). Cyclopia and defective axial patterning in mice lacking Sonic hedgehog gene function. *Nature* **383**, 407-413.

Cobb, J. and Duboule, D. (2005). Comparative analysis of genes downstream of the Hoxd cluster in developing digits and external genitalia. *Development* **132**, 3055-3067.

DasGupta, R. and Fuchs, E. (1999). Multiple roles for activated LEF/TCF transcription complexes during hair follicle development and differentiation. *Development* **126**, 4557-4568.

Dassule, H. R., Lewis, P., Bei, M., Maas, R. and McMahon, A. P. (2000). Sonic hedgehog regulates growth and morphogenesis of the tooth. *Development* **127**, 4775-4785.

Deng, C. X., Wynshaw-Boris, A., Shen, M. M., Daugherty, C., Ornitz, D. M. and Leder, P. (1994). Murine FGFR-1 is required for early postimplantation growth and axial organization. *Genes Dev.* **8**, 3045-3057.

Dolle, P., Izpisua-Belmonte, J. C., Brown, J. M., Tickle, C. and Duboule, D. (1991). HOX-4 genes and the morphogenesis of mammalian genitalia. *Genes Dev.* **5**, 1767-1776.

Dunty, W. C., Jr, Biris, K. K., Chalamalasetty, R. B., Taketo, M. M., Lewandoski, M. and Yamaguchi, T. P. (2008). Wnt3a/beta-catenin signaling controls posterior body development by coordinating mesoderm formation and segmentation. *Development* **135**, 85-94.

Feil, R., Wagner, J., Metzger, D. and Chambon, P. (1997). Regulation of Cre recombinase activity by mutated estrogen receptor ligand-binding domains. *Biochem. Biophys. Res. Commun.* **237**, 752-757.

Galceran, J., Farinas, I., Depew, M. J., Clevers, H. and Grosschedl, R. (1999). Wnt3a(-/-)-like phenotype and limb deficiency in Lef1(-/-)Tcf1(-/-) mice. *Genes Dev.* **13**, 709-717.

Gregorieff, A., Grosschedl, R. and Clevers, H. (2004). Hindgut defects and transformation of the gastro-intestinal tract in Tcf4(-/-)/Tcf1(-/-) embryos. *EMBO J.* **23**, 1825-1833.

Harada, N., Tamai, Y., Ishikawa, T., Sauer, B., Takaku, K., Oshima, M. and Taketo, M. M. (1999). Intestinal polyposis in mice with a dominant stable mutation of the beta-catenin gene. *EMBO J.* **18**, 5931-5942.

Haraguchi, R., Suzuki, K., Murakami, R., Sakai, M., Kamikawa, M., Kengaku, M., Sekine, K., Kawano, H., Kato, S., Ueno, N. et al. (2000). Molecular analysis of external genitalia formation: the role of fibroblast growth factor (Fgf) genes during genital tubercle formation. *Development* **127**, 2471-2479.

Haraguchi, R., Mo, R., Hui, C., Motoyama, J., Makino, S., Shiroishi, T., Gaffield, W. and Yamada, G. (2001). Unique functions of Sonic hedgehog signaling during external genitalia development. *Development* **128**, 4241-4250.

Haraguchi, R., Motoyama, J., Sasaki, H., Satoh, Y., Miyagawa, S., Nakagata, N., Moon, A. and Yamada, G. (2007). Molecular analysis of coordinated bladder and urogenital organ formation by Hedgehog signaling. *Development* **134**, 525-533.

Harfe, B. D., Scherz, P. J., Nissim, S., Tian, H., McMahon, A. P. and Tabin, C. J. (2004). Evidence for an expansion-based temporal Shh gradient in specifying vertebrate digit identities. *Cell* **118**, 517-528.

Hu, T., Yamagishi, H., Maeda, J., McAnally, J., Yamagishi, C. and Srivastava, D. (2004). Tbx1 regulates fibroblast growth factors in the anterior heart field through a reinforcing autoregulatory loop involving forkhead transcription factors. *Development* **131**, 5491-5502.

Huelsken, J., Vogel, R., Erdmann, B., Cotsarelis, G. and Birchmeier, W. (2001). beta-Catenin controls hair follicle morphogenesis and stem cell differentiation in the skin. *Cell* **105**, 533-545.
Hui, C. C. and Joyner, A. L. (1993). A mouse model of greig cephalopolysyndactyly syndrome: the extra-toesJ mutation contains an intragenic deletion of the Gli3 gene. *Nat. Genet.* **3**, 241-246.
Hynes, P. J. and Fraher, J. P. (2004). The development of the male genitourinary system. I. The origin of the urorectal septum and the formation of the perineum. *Br. J. Plast. Surg.* **57**, 27-36.
Ingham, P. W. and McMahon, A. P. (2001). Hedgehog signaling in animal development: paradigms and principles. *Genes Dev.* **15**, 3059-3087.
Jernvall, J., Aberg, T., Kettunen, P., Keranen, S. and Thesleff, I. (1998). The life history of an embryonic signaling center: BMP-4 induces p21 and is associated with apoptosis in the mouse tooth enamel knot. *Development* **125**, 161-169.
Johnson, R. L. and Tabin, C. J. (1997). Molecular models for vertebrate limb development. *Cell* **90**, 979-990.
Kawakami, Y., Capdevila, J., Buscher, D., Itoh, T., Rodriguez Esteban, C. and Izpisua Belmonte, J. C. (2001). WNT signals control FGF-dependent limb initiation and AER induction in the chick embryo. *Cell* **104**, 891-900.
Kawakami, Y., Rodriguez-Leon, J., Koth, C. M., Buscher, D., Itoh, T., Raya, A., Ng, J. K., Esteban, C. R., Takahashi, S., Henrique, D. et al. (2003). MKP3 mediates the cellular response to FGF8 signalling in the vertebrate limb. *Nat. Cell Biol.* **5**, 513-519.
Kengaku, M., Capdevila, J., Rodriguez-Esteban, C., De La Pena, J., Johnson, R. L., Belmonte, J. C. and Tabin, C. J. (1998). Distinct WNT pathways regulating AER formation and dorsoventral polarity in the chick limb bud. *Science* **280**, 1274-1277.
Kmita, M., Tarchini, B., Zakany, J., Logan, M., Tabin, C. J. and Duboule, D. (2005). Early developmental arrest of mammalian limbs lacking HoxA/HoxD gene function. *Nature* **435**, 1113-1116.
Kondo, T., Zakany, J., Innis, J. W. and Duboule, D. (1997). Of fingers, toes and penises. *Nature* **390**, 29.
Ladher, R. K., Wright, T. J., Moon, A. M., Mansour, S. L. and Schoenwolf, G. C. (2005). FGF8 initiates inner ear induction in chick and mouse. *Genes Dev.* **19**, 603-613.
Laufer, E., Nelson, C. E., Johnson, R. L., Morgan, B. A. and Tabin, C. (1994). Sonic hedgehog and Fgf-4 act through a signaling cascade and feedback loop to integrate growth and patterning of the developing limb bud. *Cell* **79**, 993-1003.
Lewandoski, M., Sun, X. and Martin, G. R. (2000). Fgf8 signalling from the AER is essential for normal limb development. *Nat. Genet.* **26**, 460-463.
Lin, C., Yin, Y., Long, F. and Ma, L. (2008). Tissue-specific requirements of {beta}-catenin in external genitalia development. *Development* **135**, 2815-2825.
MacArthur, C. A., Lawshe, A., Xu, J., Santos-Ocampo, S., Heikinheimo, M., Chellaiah, A. T. and Ornitz, D. M. (1995). FGF-8 isoforms activate receptor splice forms that are expressed in mesenchymal regions of mouse development. *Development* **121**, 3603-3613.
Macatee, T. L., Hammond, B. P., Arenkiel, B. R., Francis, L., Frank, D. U. and Moon, A. M. (2003). Ablation of specific expression domains reveals discrete functions of ectoderm- and endoderm-derived FGF8 during cardiovascular and pharyngeal development. *Development* **130**, 6361-6374.
Mariani, F. V., Ahn, C. P. and Martin, G. R. (2008). Genetic evidence that FGFs have an instructive role in limb proximal-distal patterning. *Nature* **453**, 401-405.
Mo, R., Freer, A. M., Zinyk, D. L., Crackower, M. A., Michaud, J., Heng, H. H., Chik, K. W., Shi, X. M., Tsui, L. C., Cheng, S. H. et al. (1997). Specific and redundant functions of Gli2 and Gli3 zinc finger genes in skeletal patterning and development. *Development* **124**, 113-123.
Mo, R., Kim, J. H., Zhang, J., Chiang, C., Hui, C. C. and Kim, P. C. (2001). Anorectal malformations caused by defects in sonic hedgehog signaling. *Am. J. Pathol.* **159**, 765-774.
Moon, A. M. and Capecchi, M. R. (2000). Fgf8 is required for outgrowth and patterning of the limbs. *Nat. Genet.* **26**, 455-459.
Moon, A. M., Boulet, A. M. and Capecchi, M. R. (2000). Normal limb development in conditional mutants of Fgf4. *Development* **127**, 989-996.
Morgan, E. A., Nguyen, S. B., Scott, V. and Stadler, H. S. (2003). Loss of Bmp7 and Fgf8 signaling in Hoxa13-mutant mice causes hypospadia. *Development* **130**, 3095-3109.
Murakami, R. and Mizuno, T. (1986). Proximal-distal sequence of development of the skeletal tissues in the penis of rat and the inductive effect of epithelium. *J. Embryol. Exp. Morphol.* **92**, 133-143.
Nakaya, M. A., Biris, K., Tsukiyama, T., Jaime, S., Rawls, J. A. and Yamaguchi, T. P. (2005). Wnt3a links left-right determination with segmentation and anteroposterior axis elongation. *Development* **132**, 5425-5436.
Nieuwenhuis, E. and Hui, C. C. (2005). Hedgehog signaling and congenital malformations. *Clin. Genet.* **67**, 193-208.
Niswander, L. (2003). Pattern formation: old models out on a limb. *Nat. Rev. Genet.* **4**, 133-143.
Niswander, L., Jeffrey, S., Martin, G. R. and Tickle, C. (1994). A positive feedback loop coordinates growth and patterning in the vertebrate limb. *Nature* **371**, 609-612.
Ogino, Y., Suzuki, K., Haraguchi, R., Satoh, Y., Dolle, P. and Yamada, G. (2001). External genitalia formation: role of fibroblast growth factor, retinoic acid signaling, and distal urethral epithelium. *Ann. N. Y. Acad. Sci.* **948**, 13-31.
Park, E. J., Ogden, L. A., Talbot, A., Evans, S., Cai, C. L., Black, B. L., Frank, D. U. and Moon, A. M. (2006). Required, tissue-specific roles for Fgf8 in outflow tract formation and remodeling. *Development* **133**, 2419-2433.
Perriton, C. L., Powles, N., Chiang, C., Maconochie, M. K. and Cohn, M. J. (2002). Sonic hedgehog signaling from the urethral epithelium controls external genital development. *Dev. Biol.* **247**, 26-46.
Riddle, R. D., Johnson, R. L., Laufer, E. and Tabin, C. (1993). Sonic hedgehog mediates the polarizing activity of the ZPA. *Cell* **75**, 1401-1416.
Seifert, A. W., Yamaguchi, T. and Cohn, M. J. (2009). Functional and phylogenetic analysis shows that Fgf8 is a marker of genital induction in mammals but is not required for external genital development. *Development* **136**, 2643-2651.
Sherman, L., Wainwright, D., Ponta, H. and Herrlich, P. (1998). A splice variant of CD44 expressed in the apical ectodermal ridge presents fibroblast growth factors to limb mesenchyme and is required for limb outgrowth. *Genes Dev.* **12**, 1058-1071.
Soriano, P. (1999). Generalized lacZ expression with the ROSA26 Cre reporter strain. *Nat. Genet.* **21**, 70-71.
Soshnikova, N., Zechner, D., Huelsken, J., Mishina, Y., Behringer, R. R., Taketo, M. M., Crenshaw, E. B., 3rd and Birchmeier, W. (2003). Genetic interaction between Wnt/beta-catenin and BMP receptor signaling during formation of the AER and the dorsal-ventral axis in the limb. *Genes Dev.* **17**, 1963-1968.
Sun, X., Lewandoski, M., Meyers, E. N., Liu, Y. H., Maxson, R. E., Jr and Martin, G. R. (2000). Conditional inactivation of Fgf4 reveals complexity of signalling during limb bud development. *Nat. Genet.* **25**, 83-86.
Sun, X., Mariani, F. V. and Martin, G. R. (2002). Functions of FGF signalling from the apical ectodermal ridge in limb development. *Nature* **418**, 501-508.
Suzuki, K., Bachiller, D., Chen, Y. P., Kamikawa, M., Ogi, H., Haraguchi, R., Ogino, Y., Minami, Y., Mishina, Y., Ahn, K. et al. (2003). Regulation of outgrowth and apoptosis for the terminal appendage: external genitalia development by concerted actions of BMP signaling. *Development* **130**, 6209-6220.
Suzuki, K., Haraguchi, R., Ogata, T., Barbieri, O., Alegria, O., Vieux-Rochas, M., Nakagata, N., Ito, M., Mills, A. A., Kurita, T. et al. (2008). Abnormal urethra formation in mouse models of Split-hand/split-foot malformation type 1 and type 4. *Eur. J. Hum. Genet.* **16**, 36-44.
Takada, S., Stark, K. L., Shea, M. J., Vassileva, G., McMahon, J. A. and McMahon, A. P. (1994). Wnt-3a regulates somite and tailbud formation in the mouse embryo. *Genes Dev.* **8**, 174-189.
Takahashi, N., Ishihara, S., Takada, S., Tsukita, S. and Nagafuchi, A. (2000). Posttranscriptional regulation of alpha-catenin expression is required for Wnt signaling in L cells. *Biochem. Biophys. Res. Commun.* **277**, 691-698.
Wang, X.-P., O'Conell, D. J., Lund, J. J., Saadi, I., Kuraguchi, M., Turbe-Doan, A., Cavallesco, R., Kim, H., Park, P. J., Harada, H. et al. (2009). Apc inhibition of Wnt signaling regulates supernumerary tooth formation during embryogenesis and throughout adulthood. *Development* **136**, 1939-1949.
Yamada, G., Satoh, Y., Baskin, L. S. and Cunha, G. R. (2003). Cellular and molecular mechanisms of development of the external genitalia. *Differentiation* **71**, 445-460.
Yamada, G., Suzuki, K., Haraguchi, R., Miyagawa, S., Satoh, Y., Kamimura, M., Nakagata, N., Kataoka, H., Kuroiwa, A. and Chen, Y. (2006). Molecular genetic cascades for external genitalia formation: an emerging organogenesis program. *Dev. Dyn.* **235**, 1738-1752.
Yamaguchi, T. P., Harpal, K., Henkemeyer, M. and Rossant, J. (1994). fgfr-1 is required for embryonic growth and mesodermal patterning during mouse gastrulation. *Genes Dev.* **8**, 3032-3044.
Yamaguchi, T. P., Bradley, A., McMahon, A. P. and Jones, S. (1999). A Wnt5a pathway underlies outgrowth of multiple structures in the vertebrate embryo. *Development* **126**, 1211-1223.
Yang, L., Cai, C. L., Lin, L., Qyang, Y., Chung, C., Monteiro, R. M., Mummery, C. L., Fishman, G. I., Cogen, A. and Evans, S. (2006). Isl1Cre reveals a common Bmp pathway in heart and limb development. *Development* **133**, 1575-1585.
Yu, K. and Ornitz, D. M. (2008). FGF signaling regulates mesenchymal differentiation and skeletal patterning along the limb bud proximodistal axis. *Development* **135**, 483-491.
Zhu, J., Nakamura, E., Nguyen, M. T., Bao, X., Akiyama, H. and Mackem, S. (2008). Uncoupling Sonic hedgehog control of pattern and expansion of the developing limb bud. *Dev. Cell* **14**, 624-632.
Zuniga, A., Haramis, A. P., McMahon, A. P. and Zeller, R. (1999). Signal relay by BMP antagonism controls the SHH/FGF4 feedback loop in vertebrate limb buds. *Nature* **401**, 598-602.

BIOLOGY OF REPRODUCTION 81, 1002–1009 (2009)
Published online before print 24 June 2009.
DOI 10.1095/biolreprod.108.070599

Effects of Diethylstilbestrol on Programmed Oocyte Death and Induction of Polyovular Follicles in Neonatal Mouse Ovaries[1]

Hannah Kim,[3] Tadaaki Nakajima,[3] Shinji Hayashi,[3] Pierre Chambon,[4] Hajime Watanabe,[5] Taisen Iguchi,[5] and Tomomi Sato[2,3]

International Graduate School of Arts and Sciences,[3] Yokohama City University, Yokohama, Japan
Institut de Génétique et de Biologie Moléculaire et Cellulaire,[4] Centre National de la Recherche Scientifique/Institut National de la Santé et de la Recherche Médicale/Université Louis Pasteur, Collège de France, Illkirch, France
The Graduate University for Advanced Studies and the Okazaki Institute for Integrative Bioscience,[5] National Institute for Basic Biology, National Institutes of Natural Sciences, Okazaki, Japan

ABSTRACT

In mice, neonatal exposure to a synthetic estrogen, diethylstilbestrol (DES), induces polyovular follicles, which contain two or more oocytes per ovarian follicle. We reported previously that the estrogen receptor beta (ESR2) mediates DES signaling in polyovular follicle induction. However, the specific mechanism of polyovular follicle induction has not yet been clarified. Folliculogenesis in rodents begins soon after birth, accompanied by programmed oocyte death and germ cell loss. In this study, the effects of DES on oocyte death and on mRNA expression of genes thought to be involved in polyovular follicle induction were analyzed during a crucial period of folliculogenesis in the ovary of C57BL/6J, *Fas*$^{lpr/lpr}$ (lacking cell death receptor, FAS), and *Esr2* knockout (*Esr2* KO) mice. Neonatal DES exposure reduced programmed oocyte death in C57BL/6J mice; however, this reduction was not observed in *Esr2* KO mice. In control *Fas*$^{lpr/lpr}$ mice, the oocyte apoptotic index was significantly lower than that in the control C57BL/6J mice. However, the polyovular follicle incidence in control 20-day-old *Fas*$^{lpr/lpr}$ mice was similar to that in the control C57BL/6J mice. Moreover, DES exposure changed mRNA expression of inhibin-alpha (*Inha*) in 2-day-old C57BL/6J mice. These results suggest that inhibition of oocyte death by DES through ESR2 may be one of the triggers for polyovular follicle induction. The FAS system is also involved in neonatal oocyte death; however, reduction of oocyte death is not sufficient for polyovular follicle induction. The combination of increased *Inha* mRNA and reduction of oocyte death in the ovaries of mice by DES through ESR2 might be correlated with polyovular follicle induction.

apoptosis, estrogen receptor, follicle, follicular development, ovary

INTRODUCTION

In mice, neonatal exposure to a synthetic estrogen, diethylstilbestrol (DES), causes various abnormalities in female reproductive organs, skeletal tissue, and muscle [1–3]. In the ovary, several morphological changes are detected, including the absence of corpora lutea, hypertrophy of interstitial tissue, and the appearance of hemorrhagic cysts [4]. Polyovular follicles, which contain two or more oocytes per follicle, are also induced in the ovaries of mice exposed to DES perinatally [5].

The actions of estrogen are mediated by estrogen receptors (ERs) ERα (ESR1) and ERβ (ESR2). In the ovary, ESR1 is localized in interstitial and thecal cells, whereas ESR2 is localized in granulosa cells [6]. DES can bind to both ESR1 and ESR2, and its affinity is higher than 17β-estradiol (E2) [7]. In a study of *Esr1* knockout (*Esr1* KO) and *Esr2* KO mice, it was shown that DES induced polyovular follicles by signaling through ESR2 [8]. Not only DES, but also E2, testosterone, and other estrogenic compounds (e.g., bisphenol-A and genistein, a phytoestrogen) induce polyovular follicles in mouse ovaries [9–11]. Jefferson et al. [11] found that induction of polyovular follicles by genistein and DES was mediated by ESR2. However, neither downstream signaling via ESR2 nor the polyovular follicle induction mechanism has been elucidated.

Polyovular follicles are frequently induced by perinatal DES exposure, and the critical period for polyovular follicle induction is Postnatal Day 3 [12]. This suggests that DES affects ovarian developmental events during the perinatal period, inducing polyovular follicles. In rodents, folliculogenesis begins soon after birth. Follicles are not yet formed in the neonatal mouse ovary, which consists of only germ cell cysts and somatic cells [13]. Germ cell cysts are cell clusters formed by the proliferation of female germ cells [13]. Cyst breakdown results in germ cell loss and initiates follicle formation. Approximately two thirds of oocytes are lost via apoptosis [14]. Genistein delays cyst breakdown and reduces oocyte death through suppression of apoptosis, and these events are thought to be essential for polyovular follicle induction in the ovary [15]. DES might affect early folliculogenesis, cyst breakdown, and formation of primordial follicles.

One hypothesis about the signals initiating cyst breakdown relates to the loss of maternal hormones in newborns after delivery. This hypothesis is based on the idea that maternal hormones protect oocytes from programmed cell death. E2, progesterone, and genistein all inhibit cyst breakdown and primordial follicle formation in newborn mouse ovaries in organ culture, supporting this hypothesis [16].

On the other hand, the signals involved in programmed oocyte death have not been elucidated. Tumor necrosis factor

[1]Supported in part by a Grant-in-Aid for Encouragement of Young Scientists from the Ministry of Education, Culture, Sports, Science, and Technology of Japan to T.S.; grants for Strategic Research Projects at Yokohama City University (grant nos. K17030, K2109, and W18005) to S.H. and T.S.; a Grant-in-Aid for Scientific Research (B) to T.I.; a Health Sciences Research Grant from the Ministry of Health, Labor, and Welfare, Japan to T.I.; and a Grant for Support of the Collaborative Study at National Institute for Basic Biology to T.S.
[2]Correspondence: Tomomi Sato, Graduate School of Nanobioscience, Yokohama City University, 22-2 Seto, Kanazawa-ku, Yokohama 236-0027, Japan. FAX: 81 45 787 2413;
e-mail: tomomi@yokohama-cu.ac.jp

Received: 15 May 2008.
First decision: 2 July 2008.
Accepted: 9 June 2009.

eISSN: 1259-7268 http://www.biolreprod.org
ISSN: 0006-3363

TABLE 1. Sequences of oligonucleotides used as primers for RT-PCR or real-time quantitative PCR.

Gene	Forward sequence (5′ to 3′)	Reverse sequence (5′ to 3′)
Esr2	GGTGATTTCGAAGAGTGGAATCTC	CCATGCCCTTGTTACTGATGTG
Fas	TTTTGCTGTCAACCATGCCA	GGTTGGTGTACCCCCATTCAT
Fasl	ATGGTTCTGGTGGCTCTGGTT	ACGGAGTTCTGCCAGTTCCTT
Tnf	AGGCAGGTTCTGTCCCTTTCA	CGCGGATCATGCTTTCTGT
Tnfr1	CACCGTGACAATCCCCTGTAA	AAGAACCCTGCATGGCAGTTA
Tnfr2	TGACACCCTACAAACCGGAAC	GTCCGAGGTCTTGTTGCAGAA
Dmrta1	TCTTGCTGGCATTGGCTTT	ACGCAGTTCAAGAGGAGAGA
Ermp1	TGTGCAGTGATGCTCGAAGTT	TCTGCGCCATTAAAGAGGAAC
Lfng	GCCACAAGGAGATGACGTTCA	CACCACATTGCCTGTGAGCTT
Bmp15	TCCTTGCTGACGACCCTACATT	GGTCAGCCGAACGATGGTATAA
Gdf9	TGGTGGACCTGCTGTTTAACCT	CCAGAAGACATGGCCTCCTTTA
Inha	CTGCTCTCAATATCTCCTTCCAAGAG	CCATGGCAGTAGTGGAAGATGATGAA
Inhba	ATCATCACCTTTGCCGAGTCA	TTCTGCACGCTCCACTACTGA
Inhbb	CCATCCAGGCCTTGTTTGA	AGCTGTCACACTGCACATCCA
Fst	TCTTCTGGCGTGCTTCTTGAA	TCCGAGATGGAGTTGCAAGAT
Ppia	AGGTCCTGGCATCTTGTCCAT	CCATCCAGCCATTCAGTCTTG

(TNF), a factor inducing apoptosis, plays various roles in the ovary, including promotion of granulosa cell proliferation [17] and induction of cell death of oocytes, granulosa cells, and luteal cells [18]. Tumor necrosis factor promotes germ cell cyst breakdown and follicle formation in neonatal rat ovary in vitro [19], and the addition of TNF reduces the primordial follicle number in the neonatal mouse ovary in vitro [20]. Ovaries from TNF receptor 1 (*Tnfr1*) or *Tnfr2* KO mice, however, do not exhibit a decrease in primordial follicles compared with wild-type (WT) mice [20]. Therefore, in mice, the effects of TNF on cyst breakdown and primordial follicle formation are still under debate. Other apoptosis-inducible factors, such as cell death receptor, FAS and FAS ligand (FASL), cause granulosa cell death in atretic follicles [21, 22]. Both *Fas* and *Fasl* mRNA are expressed in granulosa cells, and FAS is also observed in oocytes [23]. The roles of FAS and FASL in oocyte death and primordial follicle assembly, however, have not been studied. In our experience, $Fas^{lpr/lpr}$ mice (mice lacking FAS; lpr stands for "lymphoproliferation") show normal fertility and oocyte viability compared with WT animals and C57BL/6J mice, although $Fas^{lpr/lpr}$ mice die within 5 mo because of lymphomas induced by lack of apoptotic cells in lymphoid organs.

Polyovular follicles are observed in some KO mice without any hormonal treatments. Polyovular follicles are found in ovaries of double mutant growth differentiation factor 9 (*Gdf9*) bone morphogenetic protein 15 (*Bmp15*) mice ($Gdf9^{+/-}Bmp15^{-/-}$), which are oocyte-secreted factors [24]. Null mice for Lunatic fringe (*Lfng*), an important Notch signaling regulator, also show polyovular follicles [25]. A DNA-binding motif (DM) domain gene, *Dmrta1* (also known as *Dmrt4*), has unknown functions in the ovary, but the ovaries of *Dmrta1* KO mice show polyovular follicles [26]. Knockdown of *Ermp1* (also known as *Felix-ina*), which encodes a transmembrane metallopeptidase of the M28 family, causes polyovular follicles in the rat ovary [27]. Growth hormone (GH) receptor and GH-binding protein KO mice also show polyovular follicles [28]. Mice overexpressing the inhibin-α gene (*Inha*) also show a high incidence of polyovular follicles [29]. Activin INHBA- and INHBB-deficient mice also show polyovular follicles at 3 mo of age [30]. Based on these results, DES probably induces polyovular follicle formation accompanied by expression changes in these genes.

This study was aimed at examining the effects of DES on oocyte death and on the mRNA expression of genes possibly involved in polyovular follicle induction during the crucial period for formation of primordial follicles in C57BL/6J, $Fas^{lpr/lpr}$, and *Esr2* KO mice.

MATERIALS AND METHODS

Animals

Adult C57BL/6J mice (CLEA, Tokyo, Japan) were kept under 12L:12D by artificial illumination (lights on 0800–2000 h) at 23°C to 25°C. They were fed a commercial diet (MF; Oriental Yeast, Tokyo, Japan) and tap water ad libitum. This diet shows slight estrogenic activity as measured by a modified yeast-based human ESR1 bioassay [31]. All animals were maintained in accordance with the National Institutes of Health Guide for the Care and Use of Laboratory Animals. All experiments were approved by the institutional animal care committee of Yokohama City University. The day of birth was regarded as Day 0. Female pups were injected s.c. with 3 μg of DES (Sigma Chemical, St. Louis, MO) dissolved in 0.02 ml of sesame oil or the vehicle alone for 2 days (from Day 0 to Day 1).

Esr2 KO mice from a C57BL6/129Sv background were obtained by mating females heterozygous and males homozygous for *Esr2* gene disruption, as described previously [32]. Female pups of WT and *Esr2* KO mice were injected s.c. with 3 μg of DES dissolved in 0.02 ml of sesame oil or the vehicle alone from Day 0 to Day 1 for 2 days. C57BL/6J Jms slc-lpr mice (*lpr/lpr* mice; $Fas^{lpr/lpr}$) were purchased from Sankyo Labo Service Corp. (Tokyo, Japan).

STAT3 and ESR2 Immunohistochemistry

Ovaries of 1-, 2-, and 3-day-old C57BL/6J mice and 2-day-old WT, *Esr2* KO, and $Fas^{lpr/lpr}$ mice were fixed in 4% paraformaldehyde in PBS (pH 7.4) at 4°C overnight (n = 4–5). Because STAT3-positive staining was detected in the cytosol of oocytes [33], STAT3 was used as a marker of oocytes. Ovaries were embedded in paraffin and serially sectioned at 4 μm. Sections were deparaffinized, rehydrated, and microwaved for 6 min for STAT3 staining or for 8 min for ESR2 staining in a 10 mM sodium citrate buffer (pH 6.0) for antigen retrieval. To block endogenous peroxidase activity, sections were incubated in 3% H_2O_2 in ion-exchanged water for 10 min. After washing with PBS, normal goat serum (Vector Laboratories, Burlingame, CA) was used for nonspecific blocking for 30 min. Sections were then incubated with rabbit polyclonal antibody against STAT3 (Abcam, Cambridge, U.K.) at a dilution of 1:200, rabbit polyclonal antibody against ESR2 (Zymed Laboratories, San Francisco, CA) at a dilution of 1:250, or rabbit immunoglobulin G (IgG) as a negative control at 4°C overnight. Sections were incubated with biotinylated secondary antibody (Vector Laboratories) for 30 min. After washing with PBS, sections were incubated with Avidin-biotin complex (ABC) reagents (Vector Laboratories) for 30 min according to the manufacturer's protocol. A total of 1 mg/ml 3–3′-diaminobenzidine (DAB; Sigma) in PBS containing 1% H_2O_2 was used for avidin peroxidase detection, and sections were counterstained with hematoxylin. STAT3-positive cells were counted as oocytes. The nuclei of oocytes in germ cell cysts were also counted as oocytes.

Detection of Apoptotic Cells

To make precise comparisons of the same cells stained for an apoptotic signal and oocyte-specific proteins, two consecutive sections were placed on

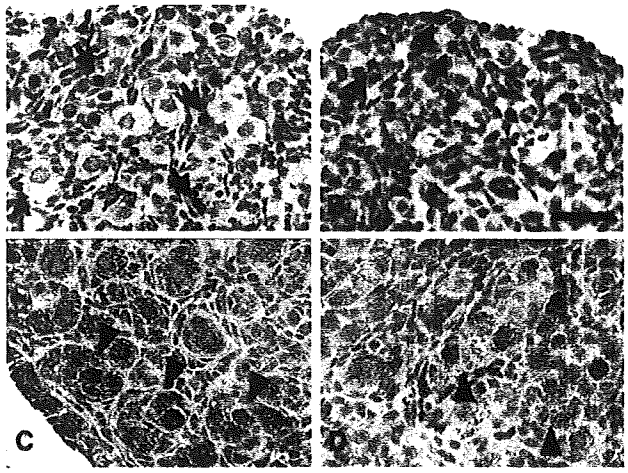

FIG. 1. TUNEL assay (**A** and **B**) and immunohistochemistry for STAT3 (**C** and **D**) of 2-day-old C57BL/6J mouse ovaries showing clusters of germ cells and surrounding somatic cells but not follicles. Neonatal DES exposure did not change the histology of ovaries compared with controls. **A** and **C** show oil controls, and **B** and **D** show DES-exposed ovaries. Arrows indicate apoptotic cells. Arrowheads indicate germ cell cysts. Bar = 50 μm.

different glass slides to form "mirror" images. These were then stained for TUNEL and STAT3, as described previously [34].

Apoptotic cells were detected by the TUNEL method. Sections were deparaffinized, dehydrated, and incubated with 20 μg/ml proteinase K (Wako Pure Chemical Industries, Osaka, Japan) in Tris-ethylenediaminetetraacetic acid buffer (TE buffer; pH 8.0) for 15 min at room temperature to strip the nuclear membrane. After washing with TE buffer, sections were incubated with 3% H_2O_2 in TE buffer for 5 min at room temperature to block endogenous peroxidase. Sections were then incubated with terminal deoxynucleotidyl transferase (TdT) buffer (30 mM Tris-HCl, 140 mM sodium cacodylate trihydrate, and 1 mM cobalt chloride, pH 7.2) for 15 min at room temperature. For the labeling reaction with TdT (Trevigen, Gaithersburg, MD), sections were incubated with 10 units of TdT and 0.0125 μM biotinylated dCTP at 37°C for 1 h, then immersed in 300 mM NaCl and 30 mM sodium citrate buffer to stop the TdT reaction. For a negative control, TdT enzyme was omitted from the reaction mixture. Bovine serum albumin (BSA) (Sigma) was used for nonspecific blocking, and sections were incubated with ABC reagent (Vector Laboratories) for 30 min according to the manufacturer's protocol. One mg/ml DAB (Sigma) in PBS containing 1% H_2O_2 and 0.1M imidazol (Sigma) was used for avidin peroxidase detection, and sections were counterstained with hematoxylin. TUNEL positive cells were counted as apoptotic cells. Five different sections of each ovary, at least 50 μm apart, were selected to count the number of oocytes and apoptotic cells. More than four animals were used in each group for immunohistochemical study.

Detection of Proliferating Cells

Two-day-old WT and *Esr2* KO mice exposed neonatally to oil or DES were injected s.c. with 1 mg/0.1 ml/10 g body weight 5-bromo-2′-deoxyuridine (BrdU; Sigma Chemical). One hour later, ovaries were fixed in 10% formalin neutral buffer solution (pH 7.4; Wako Pure Chemical Industries) at room temperature overnight (n = 4–5). Ovaries were then embedded in paraffin and serially sectioned at 4 μm. Sections were deparaffinized, dehydrated, and incubated with 0.3% H_2O_2 in methanol (Wako Pure Chemical Industries) for 30 min at room temperature to block endogenous peroxidase. After washing with 0.5% Tween 20 (Sigma Chemical) in PBS, sections were incubated in 2 N HCl for 10 min at room temperature to denature DNA. To neutralize the sections, slides were immersed twice in 0.1 M borate buffer (pH 8.5) for 5 min. Sections were then incubated with 0.1% trypsin (Sigma Chemical) in PBS for 20 min at room temperature. Bovine serum albumin was added to PBS for nonspecific blocking. Sections were then incubated with a monoclonal antibody to BrdU (Roche Applied Science, Mannheim, Germany) or mouse IgG as a negative control for 1 h at room temperature. DAB in PBS containing 1% H_2O_2 and 0.1 M imidazol was used for color development. Sections were counterstained with hematoxylin. BrdU-labeled cells were counted in five different sections from the mid portion of each ovary, at least 50 μm apart. Five animals from the WT and *Esr2* KO groups exposed to oil or DES were used to count BrdU-labeled cells.

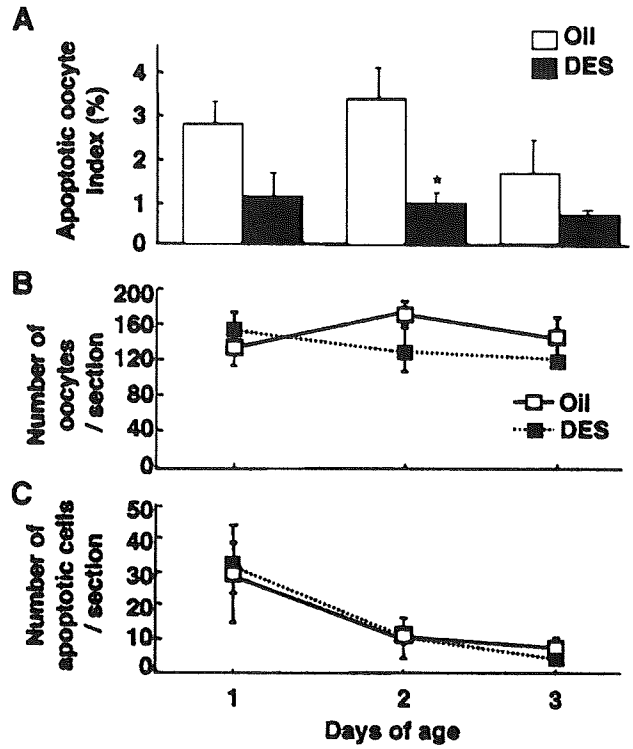

FIG. 2. Apoptotic index in oocytes (**A**), the number of oocytes per ovarian section (**B**), and the number of apoptotic cells per ovarian section (**C**) from 1- to 3-day-old, oil- or DES-exposed mice. *$P < 0.05$ compared with age-matched oil controls.

Real-Time Quantitative PCR

Total RNA was isolated from the ovaries of 2-day-old C57BL/6J mice treated neonatally with oil or DES, as well as 90-day-old C57BL/6J estrous mice, and it was reverse transcribed into cDNA using Super Script II reverse transcriptase (Invitrogen Corp., Carlsbad, CA) with 0.05 mM oligo(dT) primer (Invitrogen). Real-time PCR was carried out using a Smart Cycler II System (Takara) with SYBR Premix Ex TaqTM (Takara). Relative mRNA expression of *Esr2*, *FASL*, Fas receptor (*Fas*), *Tnf*, *Tnfrl*, *Tnfr2*, *Dmrta1*, *Ermp1*, *Lfng*, *Bmp15*, *Gdf9*, *Inha*, inhibin-βA (*Inhba*), inhibin-βB (*Inhbb*), and follistatin (*Fst*; Table 1) was determined by the second derivative method. Cyclophilin was chosen as an internal standard to control for variability in amplification due to differences in the starting mRNA concentrations. Melt-curve analysis showed a single peak for all samples. Ovaries from 5 to 10 mice were pooled for each point, and four independent experiments were carried out for each study. Data analysis was performed as described previously [35].

Statistical Analysis

Data are expressed as the mean ± standard error. Multiple comparisons, Tukey-Kramer honestly significant difference (HSD), or Dunnett post hoc tests were performed. Two-tailed Student *t*-test was used for single comparisons. A statistically significant difference was defined as $P < 0.05$.

RESULTS

Oocyte Apoptosis in Neonatal C57BL/6J Mice

In neonatal C57BL/6J mouse ovaries, apoptotic cells were observed in oocytes and somatic cells throughout the ovary, both in oil controls and DES-exposed mice (Fig. 1, A and B).

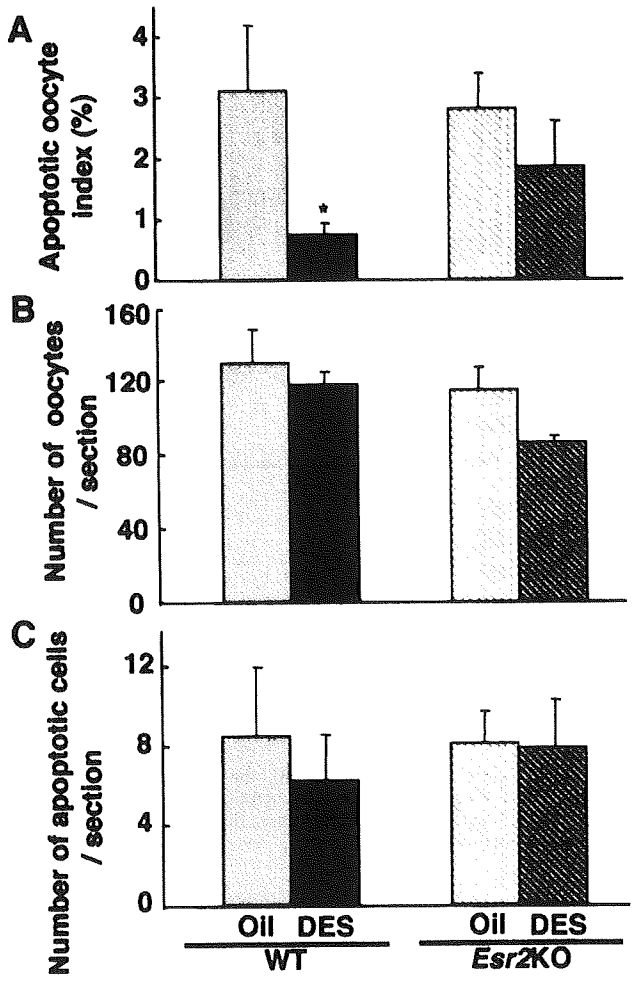

FIG. 3. Apoptotic index in oocytes (**A**), the number of oocytes per ovarian section (**B**), and the number of apoptotic cells per ovarian section (**C**) from 2-day-old WT or *Esr2* KO mice exposed neonatally to oil or DES. *$P < 0.05$ compared with age-matched oil controls.

Germ cell cysts were also observed in both control and DES-exposed mice (Fig. 1, C and D). To make precise comparisons of the same cells stained for an apoptotic signal and oocyte-specific proteins, two consecutive sections were placed on different glass slides to form mirror images. These were then stained for TUNEL and STAT3, as described in *Materials and Methods*. Neonatal DES exposure significantly decreased the apoptotic index (percentage of cells showing TUNEL staining) in oocytes of 2-day-old C57BL/6J mice (Fig. 2A). The number of apoptotic cells and oocytes in a section did not change in the oil- or DES-treated groups at any age examined (Fig. 2, B and C). BrdU-labeled cells in the ovary of 2-day-old DES-treated mice were similar to those in oil-treated mice (data not shown).

Oocyte Apoptosis in Neonatal WT or Esr2 *KO Mice*

The incidence of polyovular follicles in *Esr2* KO mice exposed neonatally to DES was lower than that in DES-exposed WT mice [8]. To determine whether inhibition of oocyte apoptosis in DES-treated mice was mediated by ESR2, TUNEL staining was performed in oil- and DES-treated WT and *Esr2* KO mice. In WT mice, DES decreased the apoptotic index, like the results seen in C57BL/6J mice; however, DES

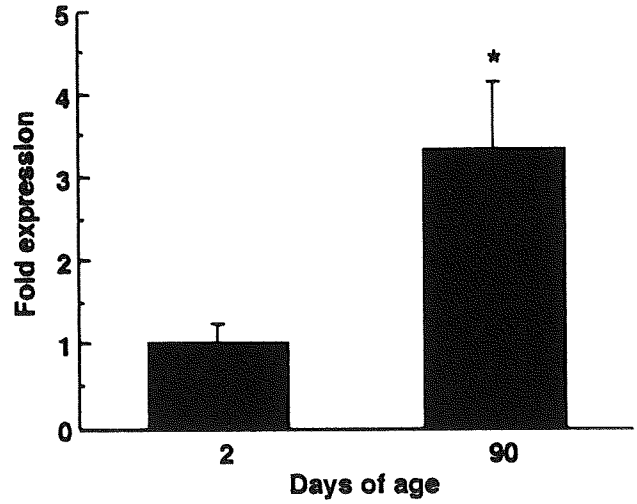

FIG. 4. Relative expression of *Esr2* mRNA in ovaries from 2-day-old and 90-day-old estrous C57BL/6J mice. *$P < 0.05$ compared with 2-day-old mice.

treatment did not change the apoptotic index in oocytes in the 2-day-old *Esr2* KO mouse ovaries (Fig. 3A). The number of apoptotic cells and oocytes in ovarian sections did not change in nither oil- or DES-treated WT and *Esr2* KO mice (Fig. 3, B and C).

Proliferating somatic cells were observed frequently in 2-day-old WT and *Esr2* KO mouse ovaries; however, proliferation of oocytes was never observed (data not shown). The number of BrdU-labeled cells did not change between WT and *Esr2* KO mice (data not shown). In addition, DES showed no effect on somatic cell proliferation in ovaries in WT and *Esr2* KO mice (data not shown).

Expression of ESR2 Protein and mRNA in 2-Day-Old C57BL/6J Mice

ESR2-positive cells were not observed by immunohistochemistry in 2-day-old, oil- or DES-exposed mice (data not shown). Expression of *Esr2* mRNA was detected in 2-day-old mouse ovaries by real-time quantitative PCR, and it was significantly increased in 90-day-old mouse ovaries (Fig. 4).

Oocyte Apoptosis and Polyovular Follicle Incidence in $Fas^{lpr/lpr}$ *Mice*

Histology of ovaries of $Fas^{lpr/lpr}$ mice was the same as C57BL6J mice, showing clusters of oocytes and surrounding somatic cells (data not shown). In the 2-day-old $Fas^{lpr/lpr}$ mouse ovary, the apoptotic index of oocytes was significantly low compared with that seen in oil-treated C57BL/6J mice (Fig. 5A). The number of oocytes in $Fas^{lpr/lpr}$ mice was similar to that in oil- and DES-exposed C57BL/6J mice (Fig. 5, B and C). The mRNA expression of genes associated with apoptosis did not change in DES-treated C57BL/6J mice versus oil controls (Fig. 5D).

Because polyovular follicle incidence was the highest in 20-day-old mouse ovary exposed neonatally to DES [8], histological observation was performed in 20-day-old $Fas^{lpr/lpr}$ mice. The incidence of polyovular follicles in oil control $Fas^{lpr/lpr}$ mice was similar to that in oil control C57BL/6J mice (Fig. 6A). The incidence of polyovular follicles in both DES-exposed $Fas^{lpr/lpr}$ mice and C57BL/6J mice was significantly higher than that in respective oil controls (Fig. 6A). The

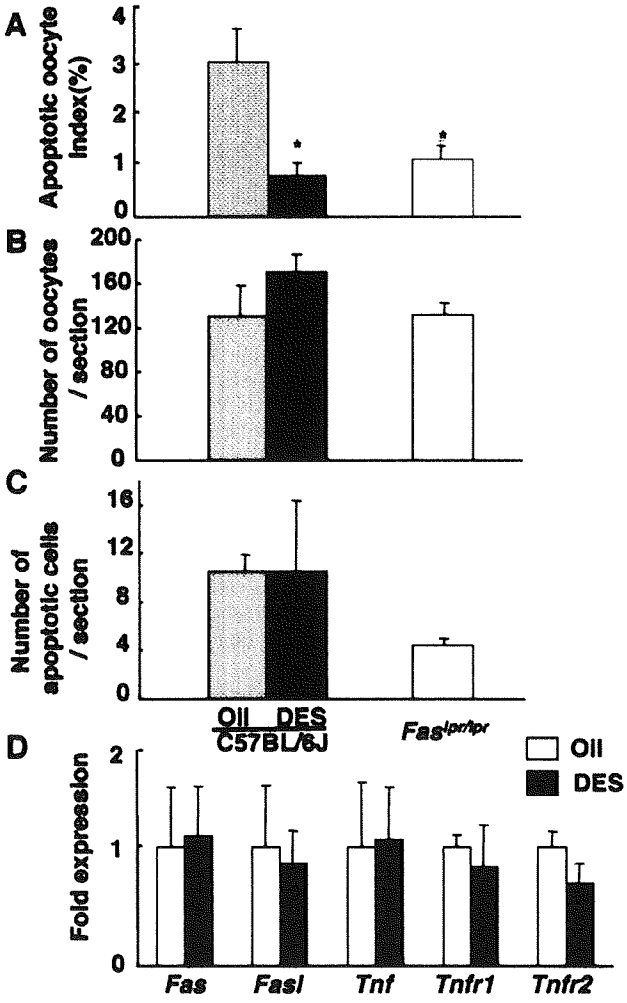

FIG. 5. Apoptotic index in oocytes (**A**), the number of oocytes per ovarian section (**B**), and the number of apoptotic cells per ovarian section (**C**) in 2-day-old C57BL/6J mice exposed neonatally to oil or DES, and 2-day-old $Fas^{lpr/lpr}$ mice. **D**) The mRNA expression of genes associated with apoptosis in 2-day-old C57BL/6J mice exposed neonatally to oil or DES. $^*P < 0.05$ compared with oil control C57BL/6J mice.

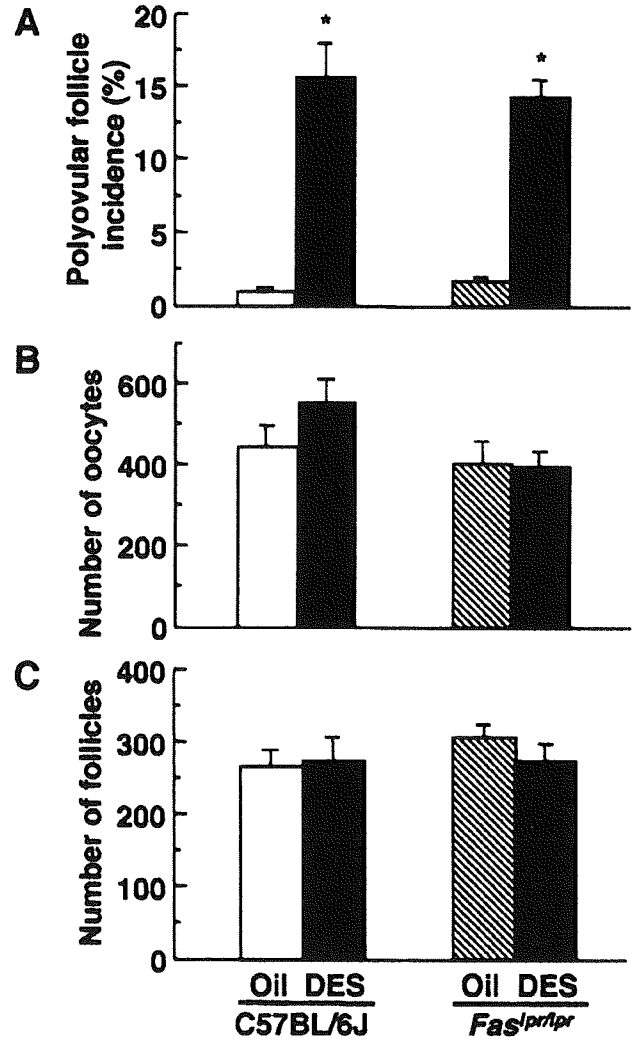

FIG. 6. Polyovular follicle incidence (**A**), the number of oocytes per ovarian section (**B**), and the number of follicles per ovarian section (**C**) in 20-day-old C57BL/6J and $Fas^{lpr/lpr}$ mice exposed neonatally to oil or DES. $^*P < 0.05$ compared with oil control mice.

number of oocytes and follicles (larger than 50 μm in diameter) in oil- or DES-exposed $Fas^{lpr/lpr}$ mice was also similar to that seen in oil- or DES-exposed C57BL/6J mice, respectively (Fig. 6, B and C).

Changes in mRNA Expression of Genes Possibly Associated with Polyovular Follicle Induction

Neonatal DES exposure significantly increased *Inha* mRNA expression in the ovaries of 2-day-old C57BL/6J mice (Fig. 7). However, expression of other genes selected as candidates of polyovular follicle formation, such as *Dmrt4*, *Fxna*, *Lfng*, *Bmp15*, *Gdf9*, *Inhba*, *Inhbb*, and *Fst* mRNAs, did not show significant change between oil- and DES-treated mice (Fig. 7).

DISCUSSION

The present study demonstrated that neonatal DES exposure lowered the oocyte apoptosis in C57BL/6J mice and WT mice but not in *Esr2* KO mice. These results suggest that DES suppresses programmed oocyte death through ESR2 and disrupts cyst breakdown. The mechanism of polyovular follicle induction by neonatal DES exposure is thought to be similar to that by genistein exposure [15]; namely, an inhibition of oocyte

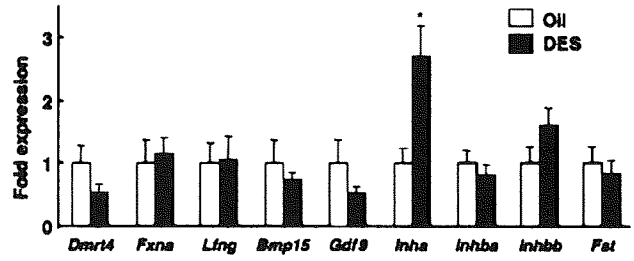

FIG. 7. Changes in the mRNA expression of genes potentially associated with polovular follicle induction in 2-day-old C57BL/6J mouse ovaries exposed neonatally to DES or oil controls. $^*P < 0.05$ compared with oil control mice.

death. *Esr2* mRNA and protein are localized in granulosa cells from Day 5 through adulthood in mice [36]. In the C57BL/6J mouse ovary, *Esr2* mRNA was detected by RT-PCR at Day 2; however, ESR2-positive cells were not observed by immunohistochemistry in the present study. Although relative expression of *Esr2* mRNA in 2-day-old mouse ovaries was significantly lower than that in 90-day-old mice, ESR2 is sufficiently expressed in the neonatal ovary, even if the protein is not detected by immunohistochemistry.

The oocyte apoptosis of $Fas^{lpr/lpr}$ mice was significantly lower than that of C57BL/6J mice, even without DES exposure. This suggests that the FAS system is a mediator of apoptotic signaling in oocytes in the neonatal mouse ovary. Indeed, *Fas*-deficient mice exhibit higher numbers of oocytes in the fetal and postnatal days [37]. *Kit*-deficient mice (Wv/Wv) exhibit oocyte depletion in the ovary; however, oocyte depletion is ameliorated in *Kit* and *Fas* double-deficient mice (Wv/Wv:$Fas^{-/-}$) [37, 38]. These reports support the idea that FAS plays an important role in oocyte death. DES exposure did not alter the mRNA expression of genes potentially associated with apoptosis, including *FASL*, *FAS*, *Tnf*, and *Tnfr* in the present study. This is consistent with the result that the total number of apoptotic cells in DES-exposed C57BL/6J mice was similar to that seen in oil-exposed mice. Thus, FASL-FAS and/or TNF-TNFR signals also could play a role in the apoptosis of somatic cells in the ovary.

Although the oocyte apoptosis in $Fas^{lpr/lpr}$ mice at Day 20 was significantly lower than that of C57BL/6J mice, the incidence of polyovular follicle was not different between these two strains. This fact suggests that a decrease in oocyte apoptosis is not the only factor in polyovular follicle formation, even though the necessity of oocyte apoptosis in the induction of polyovular follicles by DES has been reported [15]. Several studies using overexpression or deletion of apoptosis-associated genes in mice support this hypothesis. Mice overexpressing BCL2 exhibit an increase in primordial follicle number at Day 8 [39], whereas *Bcl2* deletion results in a reduction in follicle endowment [40]. Neonatal proapoptotic BCL2-associated X protein (BAX) KO mice show an increase in naked oocytes and primordial follicles compared with WT mice [41]. In contrast, loss of function of the antiapoptotic protein BCL2L1 (also known as Bcl-XL) in mice causes follicle depletion [42]. These reports indicate that several factors associated with apoptosis affect the number of oocytes or follicle endowment; however, the occurrence of polyovular follicles has never been reported. This leads us to speculate that other events are necessary for the induction of polyovular follicles besides the suppression of oocyte apoptosis, changes in oocyte number, and disruption of follicle formation.

In addition to programmed oocyte death, pregranulosa cell invasion into germ cell cysts and basement membrane remodeling are also essential events for follicle formation [14, 43]. Moreover, although both oocytes and somatic cells are important for the formation and development of follicles [44–48], the proportion of oocytes to somatic cells in the ovary is apparently critical for follicle formation. In DES-exposed, 2-day-old C57BL/6J mice, apoptotic oocytes were decreased but BrdU-labeled cells not changed compared with oil-exposed mice. This suggests that DES can alter the proportion of oocytes to somatic cells in the neonatal mouse ovary. In fact, irradiation of fetal rats results in polyovular follicles in the ovary due to severe perturbations of follicle histogenesis and massive germ cell depletion [49]. Thus, alterations in the ovarian cell population by neonatal DES exposure might affect the invasion of pregranulosa cells and basement membrane remodeling. These events need to be studied in the near future because they could be one of the triggers for polyovular follicle induction.

Polyovular follicles have been observed in ovaries of double mutant $Gdf9^{+/-}Bmp15^{-/-}$ mice [24]. In our study, DES exposure did not change the expression of *Gdf9* or *Bmp15* mRNA. *Gdf9* mRNA and protein are usually detected in oocytes [50]. $Gdf9^{-/-}$ mice are infertile, and their folliculogenesis is stopped at the primary follicle stage, suggesting that GDF9 can regulate the proliferation and differentiation of granulosa cells [51]. *Gdf9* has three newborn ovary homeobox gene (Nobox)-binding elements in the promoter region and is directly regulated by NOBOX, which is expressed in primordial and growing oocytes [45, 52, 53]. Expression of *Nobox* mRNA was not changed by DES treatment [54]; therefore, the NOBOX-GDF9 cascade is not affected by DES.

DES exposure increased *Inha* mRNA expression in mouse ovaries at Day 2, consistent with the fact that the ovaries of transgenic mice expressing the rat inhibin-α subunit gene displayed polyovular follicles [29]. Moreover, activin-deficient mice with polyovular follicles show a decrease of serum inhibin A; however, *Inha* mRNA expression of those ovaries is increased [30]. In *Esr2* KO mice, changes of *Inha* mRNA expression and polyovular follicles were not induced by neonatal DES exposure (our unpublished data). Thus, high expression of *Inha* mRNA may be correlated with the polyovular follicle induction.

Inhibin is secreted by granulosa cells and inhibits follicle-stimulating hormone (FSH) production in the pituitary. Follicle-stimulating hormone activates the *Inha* gene via an increase in cAMP [55, 56]. Follicle-stimulating hormone increases mRNA expression of *Gata4* [57]. GATA4 is activated by phosphorylation via the cAMP/protein kinase A signaling pathway. Because *Inha* has two GATA motifs in its promoter region, activated GATA4 can increase *Inha* mRNA expression [58, 59]. These reports suggest that FSH can activate *Inha* gene expression indirectly. On the other hand, neonatal DES exposure decreases pituitary and serum FSH/luteinizing hormone (LH) levels in mice at Day 6 [60]. Although the levels of FSH/LH in the serum of DES-exposed mice have not been clarified at Day 2, FSH might not be responsible for the increase in *Inha* gene expression. The other factor that may be involved in the increase of *Inha* mRNA is GDF9. GDF9 alone or with FSH increases *Inha* mRNA and promoter activity in rat granulosa cells in vitro [61], even without cAMP mediation [51]. Because our results showed that *Gdf9* mRNA was not changed by DES, involvement of GDF9 in the upregulation of *Inha* cannot be assumed. Another candidate is transforming growth factor-β (TGFB). *Inha* mRNA is positively regulated by TGFB via GATA4 interaction with *Smad3* [62]. Steroidogenic factor-1 (SF1) directly activates the *Inha* gene promoter, and the action of SF1 on the *Inha* gene is intensified by cAMP response element-binding protein [63]. The WNT signaling pathway downstream effector, β-catenin, synergizes with SF1 and activates the *Inha* promoter via formation of a transcriptional complex [64]. Neonatal exposure to estradiol benzoate or DES results in a decrease in SF1 expression in the ovary [65, 66]. Thus, it is possible that DES affects *Inha* expression through these factors.

A single injection of inhibin into the rat ovarian bursa causes an increase in the number of follicles, and activin causes follicular atresia in adult rats [67]; however, roles of inhibin and activin in the neonatal ovary are still unclear. Kipp et al. [68] showed that neonatal exposure to estrogens suppresses the mRNA expression of *Inhba*. *Inhba* deficiency induces polyovular follicles [30]. Homodimers and heterodimers of

the inhibin-β subunits act as activins. Thus, it is hypothesized that activin may play an important role in cyst breakdown, and the suppression of activin may be correlated with an induction of polyovular follicles [68]. In this study, both *Inhba* and *Inhbb* subunit genes were not altered after DES exposure. Because inhibin functionally antagonizes activin in the ovary, elevated levels of inhibin-α may suppress the activin actions in the DES-exposed ovary thorough competition for subunit assembly, such as mice overexpressing the *Inha* gene [29]. FST is also known as a competitor of activin; however, no change in *Fst* mRNA expression indicates that FST is excluded from this phenomenon. Therefore, the inhibin:activin ratio may be important in the cyst breakdown and maintenance of ovarian follicular development. A decrease of *Inhba* and/or an increase of *Inha* induced by neonatal DES exposure may affect cyst breakdown and result in polyovular follicles. Further studies are needed to examine the factors, such as TGFB and SF1, which can regulate *Inhba* and/or *Inha* subunit genes in ovaries of mice exposed neonatally to DES.

At all ages examined, the number of oocytes did not change, regardless of strain or treatment. This indicates that inhibition of oocyte death by DES does not influence the number of oocytes. Two hypotheses can be proposed to explain this result. First, oocytes could proliferate, or germ stem cells might exist in the mouse ovary. It has been believed for a long time that most mammalian species lose the capacity for oocyte proliferation during fetal development, and new oocytes never generate in the ovary. However, female flies maintain their capability for oocyte proliferation even as adults via a specialized cell population referred to as "germline stem cells" [69]. Johnson et al. [71, 72] detected proliferative germ cells in the postnatal ovary and identified bone marrow cells as a potential source of germ cells that could sustain oocyte production in adults [72]. In 2-day-old WT and *Esr2* KO mouse ovaries, BrdU-labeled oocytes were never found; therefore, it is hard to speculate on the possibility of oocyte proliferation. The second hypothesis is that DES may delay the timing of oocyte death. In mice, oocyte death peaks at Day 1 or 2, regardless of mouse strain [14]. When DES is present, oocyte death is inhibited and germ cell cysts may remain; however, once DES is metabolized, oocytes in germ cell cysts could be directed to apoptosis. Most polyovular follicles contain two or three oocytes, whereas germ cell cysts in the neonatal ovary consist of two, four, or eight oocytes [14]. This may support the idea that DES might delay oocyte death; however, further studies are needed.

Our results suggest that delay or inhibition of oocyte death and an increase of *Inha* by DES through ESR2 may be one of the triggers for polyovular follicle formation. Although FAS system is involved in neonatal oocyte death, inhibition of oocyte death is not the only factor in induction of polyovular follicles; therefore, further studies are needed to understand the molecular mechanism of polyovular follicle formation.

REFERENCES

1. Takasugi N. Vaginal cornification in persistent-estrous mice. Endocrinology 1963; 72:607–619.
2. Iguchi T. Cellular effects of early exposure to sex hormones and abnormalities of female reproduction. Int Rev Cytol 1992; 139:1–57.
3. Iguchi T, Sato T. Endocrine disruption and developmental abnormalities of female reproduction. Am Zool 2000; 40:402–411.
4. Tenenbaum A, Forsberg JG. Structural and functional changes in ovaries from adult mice treated with diethylstilbestrol in the neonatal period. J Reprod Fertil 1985; 73:465–477.
5. Iguchi T, Takasugi N. Polyovular follicles in the ovary of immature mice exposed prenatally to diethylstilbestrol. Anat Embryol 1986; 175:53–55.
6. Sar M, Welsch F. Differential expression of estrogen receptor-β and estrogen receptor-α in rat ovary. Endocrinology 1999; 140:963–971.
7. Kuiper GGJM, Carlsson B, Grandien K, Enmarkr E, Haggblad J, Nilsson S, Gustafsson JÅ. Comparison of ligand binding specificity and transcript tissue distribution of estrogen receptors α and β. Endocrinology 1997; 138:863–870.
8. Kirigaya A, Sato T, Iguchi T, Hayashi S. Involvement of MIS and ERβ in induction of polyovular follicles (PF) in mouse ovary treated with DES neonatally. Zool Sci 2004; 21:1343.
9. Iguchi T, Todoroki R, Takasugi N, Petrow V. The effects of aromatase inhibitor and a 5α-reductase inhibitor upon the occurrence of polyovular follicles, persistent anovulation, and permanent vaginal stratification in mice treated neonatally with testosterone. Biol Reprod 1988; 39:686–697.
10. Suzuki A, Sugihara A, Uchida K, Sato T, Ohta Y, Katsu Y, Watanabe H, Iguchi T. Developmental effects of perinatal exposure to bisphenol-A and diethylstilbestrol on reproductive organs in female mice. Reprod Toxicol 2002; 16:107–116.
11. Jefferson WN, Couse JF, Padilla-Banks E, Korach KS, Newbold RR. Neonatal exposure to genistein induces estrogen receptor (ER) β expression and multioocyte follicles in the maturing mouse ovary: evidence for ERβ-mediated and nonestrogenic actions. Biol Reprod 2002; 67:1285–1296.
12. Iguchi T, Takasugi N, Bern HA, Mills KT. Frequent occurrence of polyovular follicles in ovaries of mice exposed neonatally to diethylstilbestrol. Teratology 1986; 34:29–35.
13. Pepling ME, Spradling AC. Female mouse germ cell form synchronously dividing cysts. Dev Biol 1998; 125:3323–3328.
14. Pepling ME, Spradling AC. Mouse ovarian germ cell cysts undergo programmed breakdown to form primordial follicles. Dev Biol 2001; 234: 339–351.
15. Jefferson W, Newbold R, Padilla-Banks E, Pepling M. Neonatal genistein treatment alters ovarian differentiation in the mouse: inhibition of oocyte nest breakdown and increased oocyte survival. Biol Reprod 2006; 74:161–168.
16. Ying C, Jefferson WN, Newbold RR, Banks EP, Pepling ME. Estradiol, progesterone and genistein inhibit oocyte nest breakdown and primordial follicle assembly in the neonatal mouse ovary in vitro and in vivo. Endocrinology 2007; 148:3580–3590.
17. Son DK, Arai KY, Roby KF, Terranova PF. Tumor necrosis factor α (TNF) increases granulosa cell proliferation: dependence on c-Jun and TNF receptor type 1. Endocrinology 2004; 145:1218–1226.
18. Abdo M, Hisheh S, Dharmarajan A. Role of tumor necrosis factor-alpha and the modulating effect of the caspases in rat corpus luteum apoptosis. Biol Reprod 2003; 68:1241–1248.
19. Morrison LJ, Marcinkiewicz JL. Tumor necrosis factor α enhances oocyte/follicle apoptosis in the neonatal rat ovary. Biol Reprod 2002; 66:450–457.
20. Greenfeld CR, Roby KF, Pepling ME, Babus JK, Terranova PF, Flaws JA. Tumor necrosis factor (TNF) receptor type 2 is an important mediator of TNFα function in the mouse ovary. Biol Reprod 2007; 76:224–231.
21. Sakamaki K, Yoshida H, Nishimura Y, Nishikawa S, Manabe N, Yonehara S. Involvement of Fas antigen in ovarian follicular atresia and luteolysis. Mol Reprod Dev 1997; 47:11–18.
22. Roughton SA, Lareu RR, Bittles AH, Dharmarajan AM. Fas and Fas ligand messenger ribonucleic acid and protein expression in the rat corpus luteum during apoptosis-mediated luteolysis. Biol Reprod 1999; 69:797–804.
23. Dahrma SJ, Kelkar RL, Nandedkar TD. Fas and Fas ligand protein and mRNA in normal and atretic mouse ovarian follicles. Reproduction 2003; 126:783–789.
24. Yan C, Wang P, DeMayo J, DeMayo FJ, Elvin JA, Carino C, Prasad SV, Skinner SS, Dunbar BS, Dobe JL, Celeste AJ, Matzuk MM. Synergistic roles of bone morphogenetic protein 15 and growth differentiation factor 9 in ovarian function. Mol Endocrinol 2001; 15:854–866.
25. Hahn KL, Johnson J, Beres BJ, Howard S, Rawls JW. Lunatic fringe null female mice are infertile due to defects in meiotic maturation. Development 2005; 132:817–828.
26. Balciuniene J, Bardwell VJ, Zarkower D. Mice mutant in the DM domain gene Dmrt4 are viable and fertile but have polyovular follicles. Mol Cell Biol 2006; 26:8984–8991.
27. Rudaz CG, Luna F, Tapia V, Kerr B, Colgin L, Galimi F, Dissen GA, Rawlings ND, Ojeda SR. Fxna, a novel gene differentially expressed in the rat ovary at the time of folliculogenesis, is required for normal ovarian histogenesis. Development 2007; 134:945–957.
28. Slot KA, Kastelijn J, Bachelot A, Kelly PA, Binart N, Teerds KJ. Reduced rec ruitment and survival of primordial and growing follicles in GH receptor-deficient mice. Reproduction 2006; 131:525–532.

29. McMullen ML, Cho BN, Yates CJ, Mayo KE. Gonadal pathologies in transgenic mice expressing the rat inhibin α-subunit. Endocrinology 2001; 142:5005–5014.
30. Pangas SA, Jorgez CJ, Tran M, Agno J, Li X, Brown CW, Kumar TR, Matzuk MM. Intraovarian activins are required for female fertility. Mol Endocrinol 2007; 21:2458–2471.
31. Kato H, Iwata T, Katsu Y, Watanabe H, Ohta Y, Iguchi T. Evaluation of estrogenic activity in diets for experimental animals using in vitro assay. J Agric Food Chem 2004; 52:1410–1414.
32. Dupont S, Krust A, Gansmuller A, Dierich A, Chambon P, Mark M. Effects of single and compound knockouts of estrogen receptors α (ERα) and β (ERβ) on mouse reproductive phenotypes. Development 2000; 127: 4277–4291.
33. Murphy K, Carvajal L, Medico L, Pepling M. Expression of Stat3 in germ cells of developing and adult mouse ovaries and testes. Gene Expr Patterns 2005; 5:475–482.
34. Osamura RY, Watanabe K, Nakai Y, Imura H. Adrenocorticotropic hormone cells and immunoreactive beta-endorphin cells in the human pituitary gland: normal and pathologic conditions studied by the peroxidase-labeled antibody method. Am J Pathol 1980; 99:105–124.
35. Bookout AL, Mangelsdorf DJ. Quantitative real-time PCR protocol for analysis of nuclear receptor signaling pathways. Nucl Recept Signal 2003; 1:e012.
36. Jefferson WN, Couse JF, Banks EP, Korach KS, Newbold RR. Expression of estrogen receptor β is developmentally regulated in reproductive tissue of male and female mice. Biol Reprod 2000; 62:310–317.
37. Moniruzzaman M, Sakamaki K, Akazawa Y, Miyano T. Oocyte growth and follicular development in Kit-deficient Fas-knockout mice. Reproduction 2007; 133:117–125.
38. Sakata S, Sakamaki K, Watanabe K, Nakamura N, Toyokuni S, Nishimune Y, Mori C, Yonehara S. Involvement of death receptor Fas in germ cell degeneration in gonads of Kit-deficient Wv/Wv mutant mice. Cell Death Differ 2003; 10:676–686.
39. Flaws JA, Hirshfield AN, Hewitt JA, Babus JK, Furth PA. Effect of bcl-2 on the primordial follicle endowment in the mouse ovary. Biol Reprod 2001; 64:1153–1159.
40. Ratts VS, Flaws JA, Kolp R, Sorenson CM, Tilly JL. Ablation of bcl-2 gene expression decrease the number of oocytes and primordial follicles established in the post-natal female mouse gonad. Endocrinology 1995; 136:3665–3668.
41. Greenfeld CR, Pepling ME, Babus JK, Furth PA, Flaws JA. BAX regulates follicular endowment in mice. Reproduction 2007; 133:865–876.
42. Rucker EB III, Derisseau P, Wanger KU, Garrett L, Boris AW, Flaws JA, Hennighausen L. Bcl-x and Bax regulate mouse primordial germ cell survival and apoptosis during embryogenesis. Mol Endocrinol 2000; 14: 1038–1052.
43. Mazaud S, Guyot R, Guigon CJ, Coudouel N, Magueresse-Battistoni BL, Magre S. Basal membrane remodeling during follicle histogenesis in the rat ovary: contribution of proteinases of the MMP and PA families. Dev Biol 2005; 277:403–416.
44. Pangas SA, Choi Y, Ballow DJ, Zhao Y, Westphal H, Matzuk MM, Rajkovic A. Oogenesis requires germ cell-specific transcriptional regulators Sohlh1 and Lhx8. Proc Natl Acad Sci U S A 2006; 103: 8090–8095.
45. Rajkovic A, Pangas SA, Ballow D, Suzumori N, Martzuk MM. Nobox deficiency disrupts early folliculogenesis and oocyte-specific gene expression. Science 2004; 305:1157–1159.
46. Soyal SM, Amleh A, Dean J. FIGα, a germ cell-specific transcription factor required for ovarian follicle formation. Dev Biol 2000; 127:4645–4654.
47. Dissen GA, Romero C, Hirshfield AN, Ojeda SR. Nerve growth factor is required for early follicular development in the mammalian ovary. Endocrinology 2001; 142:2078–2086.
48. Parrott JA, Skinner MK. Kit-ligand/stem cell factor induces primordial follicle development and initiates folliculogenesis. Endocrinology 1999; 140:4262–4271.
49. Guittot SM, Guigon CJ, Coudouel N, Magre S. Consequences of fetal irradiation on follicle histogenesis and early follicle development in rat ovaries. Biol Reprod 2006; 75:749–759.
50. Dong J, Albertini DF, Nishimori K, Kumar TR, Lu N, Matzuk M. Growth differentiation factor-9 is required during early ovarian folliculogenesis. Nature 1996; 383:531–535.
51. Vitt UA, Hayashi M, Klein C, Hsueh AJ. Growth differentiation factor-9 stimulates proliferation but suppresses the follicle-stimulating hormone-induced differentiation of cultured granulosa cells from small antral and preovulatory rat follicles. Biol Reprod 2000; 62:370–377.
52. Choi Y, Rajkovic A. Characterization of NOBOX DNA binding specificity and its regulation of gdf9 and Pou5f1 promoters. J Biol Chem 2006; 281:35747–35756.
53. Suzumori N, Yan C, Matzuk MM, Rajkovic A. *Nobox* is homeobox-encoding gene preferentially expressed in primordial and growing oocytes. Mech Dev 2002; 111:137–141.
54. Kim H, Hayashi S, Chambon P, Watanabe H, Iguchi T, Sato T. Effects of diethylstilbestrol on ovarian follicle development in neonatal mice. Reprod Toxicol 2009; 27:55–62.
55. Turner IM, Saunders PT, Shimasaki S, Hillier SG. Regulation of inhibin subunit gene expression by FSH and estradiol in cultured rat granulosa cells. Endocrinology 1989; 125:2790–2802.
56. Mukherjee A, Park-Sarge OK, Mayo KE. Gonadotropins induce rapid phosphorylation of the 3′,5′-cyclic adenosine monophosphate response element binding protein in ovarian granulosa cells. Endocrinology 1996; 137:3234–3245.
57. Heikinheimo M, Ermolaeva M, Bielinska M, Rahman NA, Narita N, Huhtaniemi IT, Tanpanainen JS, Wilson DB. Expression and hormonal regulation of transcription factors GATA-4 and GATA-6 in the mouse ovary. Endocrinology 1997; 136:3505–3514.
58. Tremblay JJ, Viger RS. GATA factors differentially activate multiple gonadal promoters through conserved GATA regulatory elements. Endocrinology 2001; 142:977–986.
59. Tremblay JJ, Viger RS. Trascription factor GATA-4 is activated by phosphorylation of serine 261 the cAMP/Protein kinase A signaling pathway in granulose cells. J Biol Chem 2003; 278:22128–22135.
60. Halling A. Alterations in hypothalamic and pituitary hormone levels induced by neonatal treatment of female mice with diethylstilbestrol. Reprod Toxicol 1992; 6:335–346.
61. Roh JS, Bondestam J, Mazerbourg S, Kaivo-Oja N, Groome N, Ritvos O, Hsueh AJW. Growth differentiation factor-9 stimulates inhibin production and activates Smad2 in cultured rat granulosa cells. Endocrinology 2003; 144:172–178.
62. Anttonen M, Parviainen H, Kyronlahti A, Bielinska M, Wilson DB, Ritvos O, Heikinheimo M. GATA-4 is granulosa cell factor employed in inihibin-α activation by TGF-β pathway. J Mol Endocrinol 2006; 36:557–568.
63. Ito M, Park YG, Weck J, Mayo KE, Jameson JL. Synergistic activation of the inhibinα-promoter by steroidogenic factor-1 and cyclic adenosine 3,5-monophosphate. Mol Endocrinol 2000; 14:66–81.
64. Gummow BM, Winnay JN, Hammer GD. Convergence of Wnt signaling and steroidogenic factor-1 (SF-1) on transcription of the rat inhibinα gene. J Biol Chem 2003; 278:26572–26579.
65. Ikeda Y, Nagai A, Ikeda M, Hayashi S. Neonatal estrogen exposure inhibits steroidogenesis in the developing rat ovary. Dev Dyn 2001; 221: 443–453.
66. Nagai A, Ikeda Y, Aso T, Eto K, Ikeda M. Exposure of neonatal rats to diethylstilbestrol affects the expression of genes involved in ovarian differentiation. J Med Dent Sci 2003; 50:35–40.
67. Woodruff TK, Lyon RJ, Hansen SE, Rice GC, Mather JP. Inhibin and activin locally regulate rat ovarian folliculogenesis. Endocrinology 1990; 127:3196–3205.
68. Kipp JL, Kilen SM, Bristol-Gould S, Woodruff TK, Mayo KE. Neonatal exposure to estrogens suppresses activin expression and signaling in the mouse ovary. Endocrinology 2007; 148:1968–1976.
69. Trombly DJ, Woodruff TK, Mayo KE. Roles for transforming growth factor beta superfamily proteins in early folliculogenesis. Semin Reprod Med 2009; 27:14–23.
70. Deng W, Lin H. Asymmetric germ cell division and oocyte determination during Drosophila oogenesis. Int Rev Cytol 2001; 203:93–138.
71. Johnson J, Canning J, Kaneko T, Pru JK, Tilly JL. Germline stem cells and follicular renewal in the postnatal mammalian ovary. Nature 2004; 428: 145–150.
72. Johnson J, Bagley J, Skaznik-Wikiel M, Lee HJ, Adams GB, Niikura Y, Tschudy KS, Tilly JC, Cortes ML, Forkert R, Spitzer T, Iacomini J, et al. Oocyte generation in adult mammalian ovaries by putative germ cells in bone marrow and peripheral blood. Cell 2005; 122:303–315.

BIOLOGY OF REPRODUCTION 82, 194–201 (2010)
Published online before print 16 September 2009.
DOI 10.1095/biolreprod.109.077305

Influences of Sex, Incubation Temperature, and Environmental Quality on Gonadal Estrogen and Androgen Receptor Messenger RNA Expression in Juvenile American Alligators (*Alligator mississippiensis*)[1]

Brandon C. Moore,[2,3] Matthew R. Milnes,[4] Satomi Kohno,[3] Yoshinao Katsu,[5] Taisen Iguchi,[5] and Louis J. Guillette Jr.[3]

Department of Biology[3], University of Florida, Gainesville, Florida
Zoological Society of San Diego,[4] Institute for Conservation Research, Reproductive Physiology Division, Escondido, California
Okazaki Institute for Integrative Bioscience,[5] National Institute for Basic Biology, National Institutes of Natural Sciences, Okazaki, Japan

ABSTRACT

Gonadal steroid hormone receptors play a vital role in transforming ligand signals into gene expression. We have shown previously that gonads from wild-caught juvenile alligators express greater levels of estrogen receptor 1 (*ESR1*) than estrogen receptor 2 (*ESR2*). Furthermore, sexually dimorphic *ESR2* mRNA expression (female > male) observed in animals from the reference site (Lake Woodruff, FL, USA) was lost in alligators from the contaminated Lake Apopka (FL, USA). We postulated that environmental contaminant exposure could influence gonadal steroid hormone receptor expression. Here, we address questions regarding gonadal estrogen and androgen receptor (*AR*) mRNA expression in 1-yr-old, laboratory-raised alligators. What are relative expression levels within gonads? Do these levels vary between sexes or incubation temperatures? Can contaminant exposure change these levels? We observed a similar pattern of expression (*ESR1* > *AR* > *ESR2*) in ovary and testis. However, both incubation temperature and environment modulated expression. Males incubated at 33.5°C expressed greater *AR* levels than females incubated at 30°C; dimorphic expression was not observed in animals incubated at 32°C. Compared to Lake Woodruff alligators, Lake Apopka animals of both sexes showed lesser *ESR2* mRNA expression levels. Employing cluster analyses, we integrated these receptor expression patterns with those of steroidogenic factors. Elevated *ESR2* and *CYP19A1* expressions were diagnostic of alligator ovary, whereas elevated *HSD3B1*, *CYP11A1*, and *CYP17A1* expressions were indicative of testis. In contrast, *AR*, *ESR1*, and *NR5A1* showed variable expressions that were not entirely associated with sex. These findings demonstrate that the mRNA expression of receptors required for steroid hormone signaling are modified by exposure to environmental factors, including temperature and contaminants.

alligator, environment, ovary, steroid hormone receptors, testis

INTRODUCTION

Steroid hormone signaling at the cellular and molecular level is regulated by the availability of ligands, the abundance of ligand-modifying enzymes, the abundance of receptors for these ligands, and molecular response elements, such as DNA response elements and subsequently recruited cofactors. Life stage, sex, and environment modulate gonadal steroid synthesis and receptor expression, resulting in differences in endocrine signaling. Across a wide range of animals, degraded environmental quality negatively influences endocrine activities through a variety of molecular mechanisms, including nuclear receptor signaling [1]. In American alligator (*Alligator mississippiensis*) gonads, we investigated the effects of sex and the environment on sex steroid receptor mRNA expression.

Previous research from our laboratory has compared the expression of steroidogenic factors and enzymes [2], steroid receptors [3], and circulating steroid concentrations [4–6] between juvenile alligators from Lake Woodruff National Wildlife Refuge, Florida, USA, an area of minimal anthropogenic influence, and the highly polluted Lake Apopka, Florida, USA [7–9]. These data suggest that the gonads of juvenile alligators are physiologically active, that these gonads show sexual dimorphisms at both hormonal and molecular levels of analysis, and that environmental factors influence their endocrine signaling. For instance, the testes of 13-mo-old alligators expressed higher levels of nuclear receptor 5A1 (*NR5A1*, also named *SF-1*), steroidogenic acute regulatory protein (*STAR*), cytochrome P450 11A1 (*CYP11A1*), hydroxy-delta-5-steroid dehydrogenase, 3beta- and steroid delta-isomerase 1 (*HSD3B1*), and cytochrome P450 17A1 (*CYP17A1*) than the ovaries of similar-age animals [2]. Conversely, ovaries of 13-mo-old females expressed greater cytochrome P450 19A1 (*CYP19A1*, or aromatase) mRNA levels than testes. These sexually dimorphic expression patterns were observed in animals hatched from eggs collected at Lake Woodruff National Wildlife Refuge and raised in a controlled laboratory environment. Within the same study, animals hatched from eggs collected from Lake Apopka did not exhibit the same patterns of sexual dimorphism. Lake Apopka males exhibited lower relative mRNA expression of *NR5A1* and *STAR* compared to Lake Woodruff males, and no difference was detected in the relative abundance of these transcripts between

[1]Supported by NIH R21 HD047885-01 (L.J.G.); NIH R21 ES014053-01 (L.J.G.); University of Florida Opportunity Fund (L.J.G.); Howard Hughes Medical Institute Professors Program (L.J.G.); National Science Foundation and Japanese Society for the Promotion of Science OISE-0413602 (M.R.M.); Japanese Ministry of Environment (Y.K. and T.I.); and Japanese Ministry of Education, Sports, Culture, and Technology (Y.K. and T.I.).
[2]Correspondence and current address: Brandon C. Moore, Center for Bioenvironmental Research, 1430 Tulane Ave., SL-3, New Orleans, LA 70112. FAX: 504 988 6428; e-mail: bmoore2@tulane.edu

Received: 3 March 2009.
First decision: 1 April 2009.
Accepted: 14 July 2009.

eISSN: 1529-7268 http://www.biolreprod.org
ISSN: 0006-3363

TABLE 1. Quantitative real-time PCR primers for alligator steroid receptors.

Gene	Primers[a] (5′-3′)	Anneal temp. (C°)	Product size (bp)	Accession no.
ESR1	F: AAGCTGCCCCTTCAACTTTTTA R: TGGACATCCTCTCCCTGCC	66.5	72	AB115909
ESR2	F: AAGACCAGGCGCAAAAGCT R: GCCACATTTCATCATTCCCAC	66.0	72	AB115910
AR	F: TGTGTTCAGGCCATGACAACA R: GCCCATTTCACCACATGCA	67.5	103	AB186356

[a] F, Forward; R, Reverse.

Lake Apopka males and females. In addition, expression levels of *CYP11A1* and *HSD3B1* mRNAs were not different between Lake Apopka males and females. This lack of sexual dimorphisms was associated with greatly increased posthatching mortality in Lake Apopka animals when compared to Lake Woodruff animals. These results support the hypothesis that the effects of poor environmental quality experienced by the mother are transmitted through her eggs to her offspring and that physiological changes in offspring can be observed without direct exposure to a contaminated environment during incubation or posthatching.

Recently, our laboratory reported sexually dimorphic expression of estrogen receptor mRNA in the gonads of wild-caught juvenile alligators in Lake Woodruff [3]. Juvenile alligators from Lake Apopka did not exhibit sexually dimorphic expression of estrogen receptor mRNA. It was unclear, however, if the absence of sexual dimorphism resulted from posthatching environmental exposure to xenobiotics or from developmental effects caused by differences in egg incubation temperature or maternal contribution to the embryonic environment.

In the current study, we address a series of fundamental questions regarding the effects of egg incubation temperature, sex, and environmental quality on the expression of sex steroid receptor mRNA in the gonad. The sex of all crocodilians is determined by incubation temperature during a critical window of embryonic development. Previous studies using eggs from these populations have shown that 30°C incubation produces only females, 33.5°C produces only males, and 32°C produces both males and females [10]. First, we ask what are the proportions of estrogen receptor α (*ESR1*), estrogen receptor β (*ESR2*) and androgen receptor (*AR*) mRNA expression within gonads of each sex? Second, how do these proportions vary between ovaries and testes produced at different temperatures versus ovaries and testes produced at the same temperature? Third, are there differences in expression level between ovaries and testes of alligators hatched from eggs collected at sites of differing environmental quality?

Finally, to expand our understanding of steroid signaling in these juvenile animals, we address associations between the mRNA expression of steroid receptors, regulators of steroidogenesis, and steroidogenic enzymes. To this end, we employ cluster analysis to identify novel, multivariate patterns in the data sets [11]. This technique suspends the use of experimental independent variables and finds inherent patterns of mRNA expression in the data set, forming de novo groups based on similarities in gene expression profiles. These de novo groupings of individual animals with similar expression profiles are employed to define and statistically test relationships that are not apparent when animals are clustered by experimentally defined, independent variables alone. These patterns help us to understand a "gene expression landscape" within the experiment and to identify variability in response or gene expression plasticity between the clusters.

MATERIALS AND METHODS

Experimental Design and Animal Care

All fieldwork was conducted under permits from the Florida Fish and Wildlife Conservation Commission and the U.S. Fish and Wildlife Service (permit WX01310). All work involving alligators was performed under the guidelines specified by the Institutional Animal Care and Use Committee at the University of Florida. Egg collection, handling, and incubation methods have been published previously in detail [2, 12]. In brief, soon after oviposition, six complete clutches of eggs were collected from Lake Apopka and Lake Woodruff National Wildlife Refuge during June 2001. At least one egg per clutch was opened to confirm the embryonic stage of development according to criteria set forth by Ferguson [13]. All eggs were incubated at 32°C until assigned to their respective incubation cohort at stage 19, which precedes the thermosensitive period of sex determination.

Viable eggs, as determined by candling, were allocated into one of two study designs. The first study design used only eggs from Lake Woodruff. In this design, 13 eggs were incubated at a female-producing temperature (30°C), and 17 eggs were incubated at a male-producing temperature (33.5°C). These groups were assembled from nine different clutches, with a maximum of three eggs from any clutch at either incubation temperature. The imbalance in sample size is an artifact of using these animals in several developmental studies, one of which required additional males. The second study design consisted of 60 eggs from Lake Apopka and 60 eggs from Lake Woodruff, all incubated at 32°C, a temperature that produces males and females. These groups were assembled using 10 eggs from each of six clutches collected from each study site, as described previously [2].

Incubation of Lake Woodruff eggs at 30 and 33.5°C resulted in 92% and 94% hatch rates, respectively. Hatching success and posthatching mortality from eggs incubated at 32°C have been published previously [2]. In summary, 90% of eggs from Lake Woodruff and 80% of eggs from Lake Apopka hatched. After hatching, alligators were web-tagged and housed in tanks within a greenhouse enclosure under natural lighting for 13 mo at the University of Florida. Animals were fed commercial alligator chow (Burris Mill and Feed) ad libitum. Health was checked daily, and water changes were performed every other day. Sex, as determined by visual inspections of gonad morphology and the presence or absence of oviducts at necropsy, was true to incubation temperature expectations for all animals. At necropsy, 100% (n = 12) of 30°C females and 81% (n = 13) of 33.5°C putative males survived 13 mo. In the 32°C cohort, only 66% of the animals that hatched from Lake Apopka eggs survived to 13 mo of age, compared to 96% of animals that hatched from eggs obtained from Lake Woodruff. This mortality was most extreme in females from Lake Apopka, which exhibited a 40% survival rate. At necropsy, Lake Woodruff was represented by 33 females and 19 males, whereas Lake Apopka was represented by 8 females and 19 males. Before necropsy, body mass (BM), snout-vent length (SVL), and total length (TL) were measured. Condition indices (CI) were calculated for each animal by dividing BM by SVL^3 (i.e., the SVL CI) or by TL^3 (i.e., the TL CI).

Tissue Collection, RNA Isolation, and Quantitative Real-Time PCR

At necropsy, gonads were removed, flash-frozen in liquid nitrogen, and stored at −80°C until RNA extraction was performed. RNA isolation and reverse transcription procedures have been described previously in detail [2]. Quantitative real-time PCR has been used to measure mRNA expression of each gene of interest in the American alligator [3, 14, 15], and primer sequence information, annealing temperatures, and accession numbers are reported in Table 1. Quantitative real-time PCR of steroid receptors (*ESR1*, *ESR2*, and *AR*) was performed in the MyiQ single-color detection system (Bio-Rad) following the manufacturer's protocol using iQ SYBR Green Supermix (Bio-Rad) in triplicate reaction volumes of 15 μl with 2 μl of RT product and specific primer

pairs. Expression levels of steroid receptor mRNA were calculated using gene-specific absolute standard curves, which contain the target cDNA at known concentrations. The use of absolute standard curves allows statistical comparisons of mRNA expression levels of different genes within and among samples. Measurements of steroidogenic factors (*NR5A1* and *STAR*) and steroidogenic enzymes (*CYP11A1*, *HSD3B1*, *CYP17A1*, and *CYP19A1*) were performed using relative standard curves of serially diluted cDNA as previously reported [2]. Values for each measured steroidogenic factor or enzyme mRNA expression were normalized to a mean female expression level of one. All sample means were normalized using ribosomal protein L8 (*Rpl8*) expression [2, 15].

Statistical Analysis

JMP for Windows (version 7.0.2; SAS Institute) was used for statistical analyses. To achieve homogeneous variances, morphometric data were log transformed and gene expression ratios were arcsin transformed, as needed. Significance for all tests was set at $P < 0.05$. One-way ANOVA was used to compare relative expression of steroid receptors within a gonad. Unpaired Student *t*-tests were used to compare means from females produced at 30°C to means from males produced at 33.5°C. The eggs from Lake Woodruff used in the two study designs did not originate from the same clutches; therefore, statistical comparisons between incubation temperatures within a sex (e.g., high-temperature vs. intermediate-temperature males) could not be made. Two-way ANOVA was used to compare the effects of sex and lake of origin among alligators incubated at 32°C, and least square means were analyzed using Tukey-Kramer post hoc comparisons. Significant differences by two-way ANOVA were statistically analyzed further using independent *t*-tests to identify sexual or lake-of-origin dimorphic expressions.

Hierarchical/agglomerative cluster analysis of mRNA expression data was performed using Ward linkage clustering to explore relationships in mRNA expressions between alligators of each study. Before clustering, mRNA expression data were standardized so that all variables had a mean of zero and an SD of one. Elbow criteria were used to determine the number of clusters from scree plots (not shown). Cluster analyses produced matrices of relative gene expression levels, presented here in gray-scale, colorimetric gradients, with dark squares denoting high expression levels and light squares denoting low expression levels. This expression matrix is in conjunction with adjacent distance dendrograms showing relationships based on mRNA expression similarities for individual animals in the horizontal axis and hierarchical clustering of similar gene expressions between all animals in the vertical axis. Clusters derived from the analysis were used as independent variables to reexamine the mRNA expression data using one-way ANOVA, followed by Tukey-Kramer post hoc comparisons when applicable. Pairwise linear correlation analyses were performed to further investigate specific relationships between gene expressions and are reported along with corresponding Pearson *r* values.

RESULTS

Body Morphometrics

Body mass, snout-vent length, total length, SVL CI, and TL CI were not different between 30°C females and 33.5°C males (Fig. 1, A, C, E, G, and I). Lake Apopka animals had greater body mass, snout-vent length, and total length than Lake Woodruff animals at 32°C, but within each lake no difference between sexes was detected (lake effect, $P < 0.001$ for each measurement) (Fig. 1, B, D, and F). Whereas the SVL CI did not vary by lake or sex, the TL CI was different between both

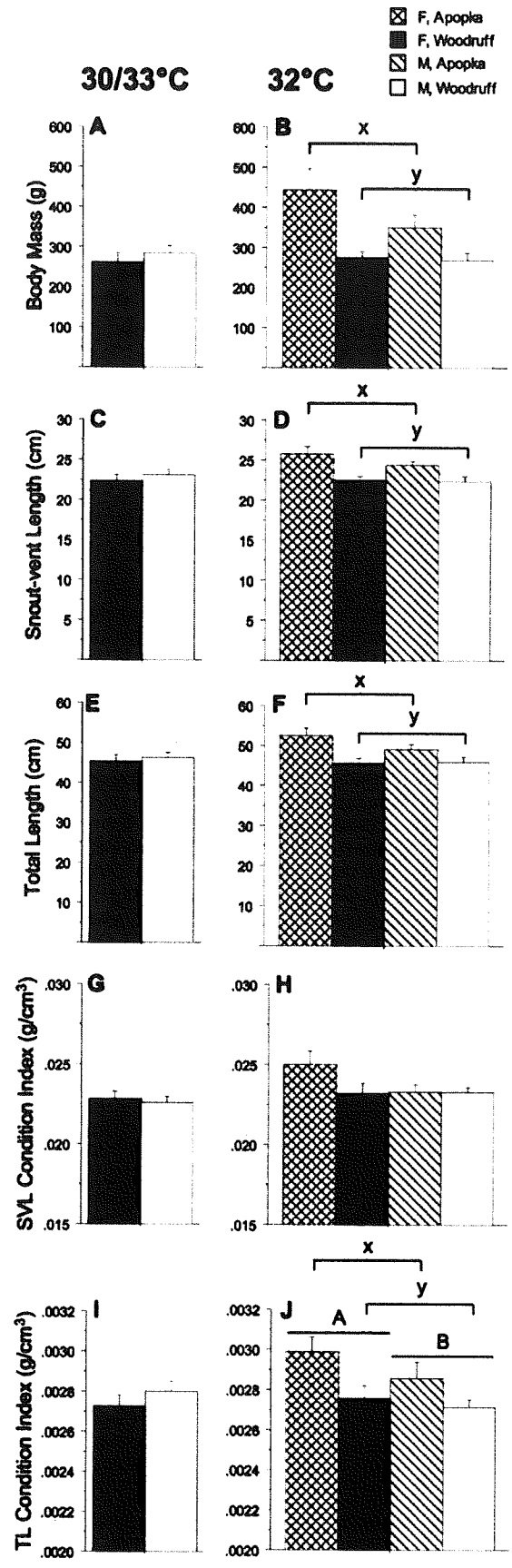

FIG. 1. Body morphometrics measurements from 13-mo-old alligators. Incubation periods were 30 or 33.5°C (**A**, **C**, **E**, **G**, and **I**) and 32°C (**B**, **D**, **F**, **H**, and **J**). Crosshatched bars are Lake Apopka females (F), and black bars are Lake Woodruff females. Diagonal lined bars are Lake Apopka males (M), and white bars are Lake Woodruff males. Bars represent the mean ± SEM for body mass (**A** and **B**), snout-vent length (**C** and **D**), and total length (**E** and **F**). Condition indices (body mass/length measurement^3) were calculated using either snout-vent length (SVL; **G** and **H**) or total length (TL; **I** and **J**). In **J**, an uppercase A and B over bars denotes a significant sex effect; in **B**, **D**, **F**, and **J**, a lowercase x and y over bars denotes a significant lake-of-origin effect.

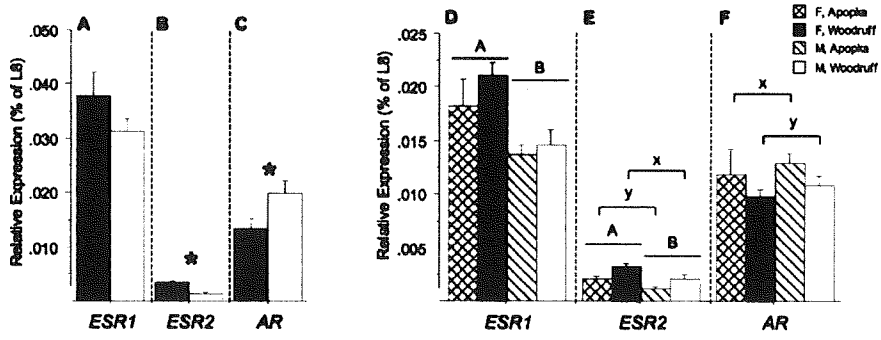

FIG. 2. Mean (± SEM) mRNA expression of *ESR1* (**A** and **D**), *ESR2* (**B** and **E**), and *AR* (**C** and **F**) in gonads of 13-mo-old alligators incubated at 30 or 33.5°C (**A–C**) or at 32°C (**D–F**). Crosshatched bars are Lake Apopka females (F), and black bars are Lake Woodruff females. Diagonal lined bars are Lake Apopka males (M), and white bars are Lake Woodruff males. In **A–C**, asterisks (*) denote a significant difference in expression between sexes. In **D–F**, an uppercase A or B over bars denotes a sex effect, and a lowercase x or y over brackets denotes a lake-of-origin effect. In **A–C** and **D–F**, respectively, expression measurements separated by dotted lines are proportional. L8, ribosomal protein L8 (*Rpl8*).

lake and sex (lake effect: $P = 0.01$; sex effect, $P = 0.02$) (Fig. 1, H and J).

Steroid Receptor Expression

Detectable levels of *ESR1*, *ESR2*, and *AR* mRNA expression were measured in ovaries and testes. The mRNA expression levels of steroid receptors within each gonad exhibited the pattern *ESR1* > *AR* > *ESR2* in all incubation groups except Lake Apopka males, in which *ESR1* = *AR* > *ESR2*. The expression of *ESR1* mRNA was not different between 33.5°C males and 30°C females, whereas *ESR2* mRNA expression was greater in ovaries than in testes and *AR* expression was greater in testes than in ovaries ($P = 0.2$, $P < 0.001$, and $P = 0.03$, respectively) (Fig. 2, A–C).

In animals incubated at 32°C, sex and lake of origin had significant interactions on expression of *ESR1*, *ESR2*, and *AR* mRNA ($P < 0.001$ for each) (Fig. 2, D–F). *ESR1* and *ESR2* mRNA expression was greater in ovary than in testis (sex effect, $P < 0.001$ for both) (Fig. 2, D and E). Gonads of Lake Woodruff animals expressed greater *ESR2* mRNA levels compared to Lake Apopka animal gonads (two-way ANOVA: lake effect, $P = 0.002$) (Fig. 2E). Conversely, Lake Apopka animal gonads expressed greater amounts of *AR* mRNA than Lake Woodruff animal gonads (two-way ANOVA: lake effect, $P = 0.05$) (Fig. 2F).

Upon further refinement of statistical analysis by independent *t*-tests, *ESR2* expression levels were different within each sex, with greater expression levels in Lake Woodruff males and females when compared to Lake Apopka animals of the same sex ($P = 0.001$ and 0.03, respectively). Furthermore, within animals from each lake, female *ESR2* expression levels were greater than male levels ($P = 0.004$ for both Lake Woodruff and Lake Apopka animals). In contrast, lake-of-origin differences were not observed in *AR* expression levels (independent *t*-tests: $P = 0.12$ and 0.21 for males and females, respectively) as observed by two-way ANOVA.

Steroidogenic Gene Expression

The expression of *NR5A1* mRNA was not different between 30°C females and 33.5°C males ($P = 0.07$) (Fig. 3A), whereas expression of *STAR*, *CYP11A1*, *HSD3B1*, and *CYP17A1* was greater in testes than in ovaries ($P < 0.001$ for each) (Fig. 3, B–E). On the other hand, *CYP19A1* mRNA expression was much greater in ovary relative to testis ($P < 0.001$) (Fig. 3F).

Multivariate Cluster Analysis of Individual Animals by mRNA Expression

Cluster analysis of females and males from 30 and 33.5°C, respectively, yielded five clusters of animals (Fig. 4, numbered clusters defined by horizontal lines on the matrix). The first node of the dendrogram of individual alligators separated males from females. Females further divided into two clusters, whereas males divided into three clusters (Fig. 4 and Table 2).

The ANOVA of the transcript level data by clusters and subsequent post hoc comparisons revealed differing expression patterns among the clusters (Table 2). The dendrogram of mRNA expression patterns divided into three groups (Fig. 4, groups defined by vertical lines on the matrix). Post hoc analysis showed that *ESR2* and *CYP19A1* mRNA expression levels displayed sexually dimorphic patterns, with females exhibiting elevated mRNA expressions. The *AR* and *ESR1* mRNA expression group had roughly sex-equivalent mRNA expressions. Male clusters exhibited considerably more variation in *HSD3B1*, *STAR*, *NR5A1*, *CYP11A1*, and *CYP17A1* mRNA levels compared to female clusters. Transcript levels in cluster 3 were similar to those in female clusters, whereas

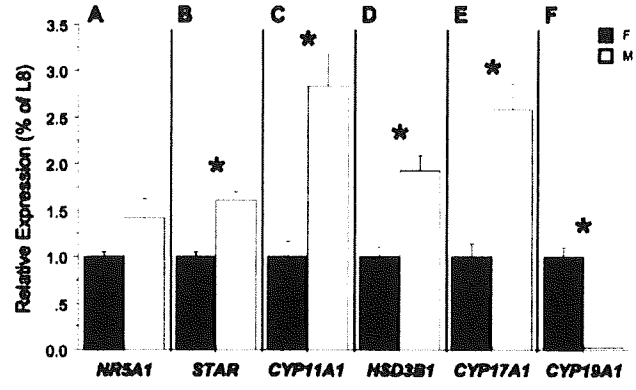

FIG. 3. Mean (± SEM) mRNA expression of (**A**) *NR5A1*, (**B**) *STAR*, (**C**) *CYP11A1*, (**D**) *HSD3B1*, (**E**) *CYP17A1*, and (**F**) *CYP19A1* in gonads of 13-mo-old, 30 or 33.5°C incubated alligators. Black bars represent females (F), and white bars represent males (M). Asterisks (*) denote a significant difference in expression between sexes. Expression measurements are not proportionally comparable. L8, ribosomal protein L8 (*Rpl8*).

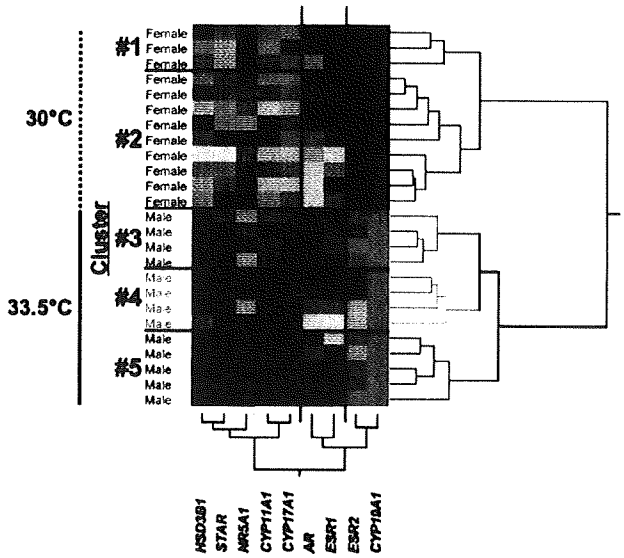

FIG. 4. Hierarchical cluster analysis of mRNA expression data from gonads of 13-mo-old Lake Woodruff alligators incubated at 30°C (vertical dotted line) or 33.5°C (vertical solid line) using Ward linkage clustering. The gray-scale, colorimetric gradient matrix displays lower expression in lighter colors and higher expressions in darker colors. Dendrograms show distance scales for individual animals in the horizontal and mRNA expressions in the vertical. Sex of individual animals is noted to the left of matrix. Horizontal lines separate numbered clusters. Vertical lines separate groups of similar gene expressions.

clusters 4 and 5 showed elevated, but variable, mRNA expressions of these steroidogenic factors.

Cluster analysis of males and females from 32°C yielded four clusters of animals (Fig. 5, numbered clusters defined by horizontal lines on the matrix). The first node of the dendrogram of individual alligators segregated all male alligators except two and included one female. Relatively equal proportions of male alligators from Lake Woodruff and Lake Apopka populated clusters 1 and 2. Clusters 3 and 4 were predominantly female, with the majority of Lake Woodruff females allocated to cluster 4, whereas Lake Apopka females distributed relatively equally between clusters 3 and 4 (Fig. 5 and Table 3).

Significant differences in mRNA expressions between clusters of animals incubated at 32°C were also observed, with post hoc analysis showing a variety of sex-related expression dimorphisms (Table 3). Cluster analysis defined four groups of mRNA expression (Fig. 5, groups defined by vertical lines on the matrix). Expression of *ESR1*, *ESR2*, and *CYP19A1* grouped as sexually dimorphic and female-elevated. The female-only cluster 4 had greater *ESR1*, *ESR2*, and *CYP19A1* mRNA expression when compared to all other clusters, including cluster 3, which was composed of 82% females. Notably, the *ESR1* mRNA expression level for the female-rich cluster 3 was lower than that for the mostly male cluster 2 and not different from the that for the all-male cluster 1. Expression levels of *AR*, *STAR*, and *NR5A1* mRNA varied between clusters, but in a non-sexually dimorphic manner. Compared to female-biased clusters, *HSD3B1*, *CYP11A1*, and *CYP17A1* mRNA expression levels were greater in the male-biased clusters. These steroidogenic enzymes had similar mRNA expression patterns, in which the mostly male cluster 2 displayed the greatest expressions, followed by the all-male cluster 1, and the lowest expression levels were observed in the all-female clusters.

DISCUSSION

Alligators lack sex chromosomes [16], and sex is determined by the temperature experienced during incubation in ovo [10]. Therefore, each embryo putatively has an equal potential to develop either testes or ovaries that produce sex-appropriate gene expressions. The sexually dimorphic mRNA expressions of steroidogenic factors and enzymes from gonads of Lake Woodruff animals incubated at 30 or 33.5°C reported here (Fig. 3) are similar to those reported previously in laboratory-raised Lake Woodruff animal ovaries and testes incubated at 32°C [2]. The one exception is *NR5A1* expression dimorphism observed in the 32°C cohort, but not in the 30 or 33.5°C cohort. These results support a hypothesis that variation in incubation temperature does not markedly effect the establishment of sex-specific mRNA expressions within gonads of a given sex.

In contrast to sexually dimorphic expressions of steroidogenic factors and enzymes observed in these gonads, the expression of estrogen and androgen receptor mRNA in ovary and testis did not present as pronounced sex-specific differences (Fig. 2). Measurement of gonadal steroid receptor mRNA expression levels in 13-mo-old alligators revealed relatively consistent expression patterns, regardless of sex or incubation temperature. In testis or ovary, the level of *ESR1* mRNA expression was greatest, whereas *AR* mRNA expression was intermediate and *ESR2* mRNA expression was lowest. The exception to this pattern was Lake Apopka males incubated at 32°C: These males exhibited equivalent *ESR1* and *AR* mRNA expression. Our laboratory has demonstrated previously a similar estrogen receptor mRNA expression pattern of *ESR1* > *ESR2* mRNA in gonads of wild-caught Lake Woodruff juvenile alligators approximately 5–7 yr of age [3]. This present study is the first to report gonadal *AR* mRNA

TABLE 2. Tukey-Kramer HSD post-hoc analysis of mRNA expressions from gonads of alligators from Lake Woodruff, incubated at 30°C (Female) and 33.5°C (Male).

	mRNA transcript†									Sex	
Cluster no.*	*HSD3B1*[a]	*STAR*[a]	*NR5A1*[a]	*CYP11A1*[a]	*CYP17A1*[a]	*AR*[b]	*ESR1*[a]	*ESR2*[c]	*CYP19A1*[a]	Male (33.5°C)	Female (30°C)
1	B,C	C	B	B	C	A,B	A	A,B	A	-	3
2	C	C	B	B	C	B	B	A	A	-	9
3	B,C	B	B	B	C	A	B	B	B	4	-
4	B	B,C	B	A	A	A,B	B	B	B	4	-
5	A	A	A	A	B	A,B	B	B	B	5	-

* Derived from hierarchical cluster analysis (Fig. 4).
† Uppercase letters represent differing Tukey-Kramer HSD post-hoc levels between clusters within each mRNA transcript.
[a] ANOVA $P < 0.001$.
[b] ANOVA $P = 0.047$.
[c] ANOVA $P = 0.002$.

expression levels that are intermediate in relation to those of *ESR1* and *ESR2*. In support of our findings, newborn mouse ovary *ESR1* expression is approximately 17-fold greater than that of *ESR2* [17].

Taking into account this expression-level hierarchy of estrogen and androgen receptors, we did observe sexually dimorphic steroid receptor expressions. In Lake Woodruff animals incubated at 30 or 33.5°C, *ESR2* mRNA expression was greater than in ovary than in testis; however, *ESR1* expression was not sexually dimorphic. A similar pattern of sexually dimorphic *ESR2* expression has been observed in gonads of wild-caught Lake Woodruff animals [3]. Additionally, in the present study, *AR* mRNA expression was greater in testes than in ovaries. In the 32°C incubation cohort, irrespective of lake of origin, these ovaries expressed greater levels of both *ESR1* and *ESR2* when compared to testes, whereas *AR* did not differ by sex. Gonads from Lake Woodruff animals, irrespective of sex, expressed higher levels of *ESR2* mRNA. Two-way ANOVA showed a lake-of-origin difference in *AR* expression levels, with greater expression levels in Lake Apopka animals, but subsequent independent *t*-tests by sex did not show similar differences. Therefore, the biological significance of this difference requires further examination.

Our findings support a hypothesis that sex, differing incubation temperatures, and environmental quality may influence steroid receptor expression, though to a lesser degree than that of the relative overall *ESR1*, *ESR2*, and *AR* level hierarchy observed in both ovary and testis. On average, estrogen receptor mRNA expressions were greater in ovaries than in testes. Androgen receptor expression was sexually dimorphic between 30 and 33.5°C gonads, but not between 32°C gonads. The environmental exposures of these 13-mo-old animals were only through maternal contribution to the egg, the oviductal environment, and a brief exposure to the nesting materials. Therefore, differences in *ESR2* mRNA expression observed at dissection are contingent on factors present well before these tissues were collected and may be organizational alterations with long-term impacts on gonadal functioning.

In the present study, we measured receptor expressions from gonad homogenates. Currently, the distribution of these steroid receptors within alligator gonads is unknown; therefore, relatively small dimorphic expressions from whole-gonad homogenates may translate into larger differences in expression in specific gonad compartments or cell types. In light of this provision, we propose that both estrogen and androgen signaling are active and equally necessary for appropriate function of juvenile alligator ovary and testis.

Literature evaluating steroid receptor expressions between sexes from nonmammalian vertebrate studies is sparse and usually focuses on embryonic development [18, 19]. AR immunoreactivity has been observed in granulosa, theca, and fibroblast cells of chicken ovarian follicles [20] and in Sertoli, Leydig, and myeloid cells of chicken and duck testes [21]. During development, *AR* mRNA is expressed in the left chicken ovary at higher levels than in testis, and *AR* levels increase in both ovary and testis before hatching [22]. Antagonism of androgen signaling in embryonic chicken ovary by flutamide treatment results in a disorganized cortex; proper ovarian development is rescued by cotreatment with either testosterone or estradiol [22]. Flutamide treatment was shown to decrease aromatase expression, leading to a hypothesis that androgen-*AR* signaling may regulate aromatase expression in the embryonic ovary. In posthatchling quail, turkey, duck, and goose gonads, *ESR1* mRNA expression is not sexually dimorphic, in spite of concomitant ovarian aromatase expres-

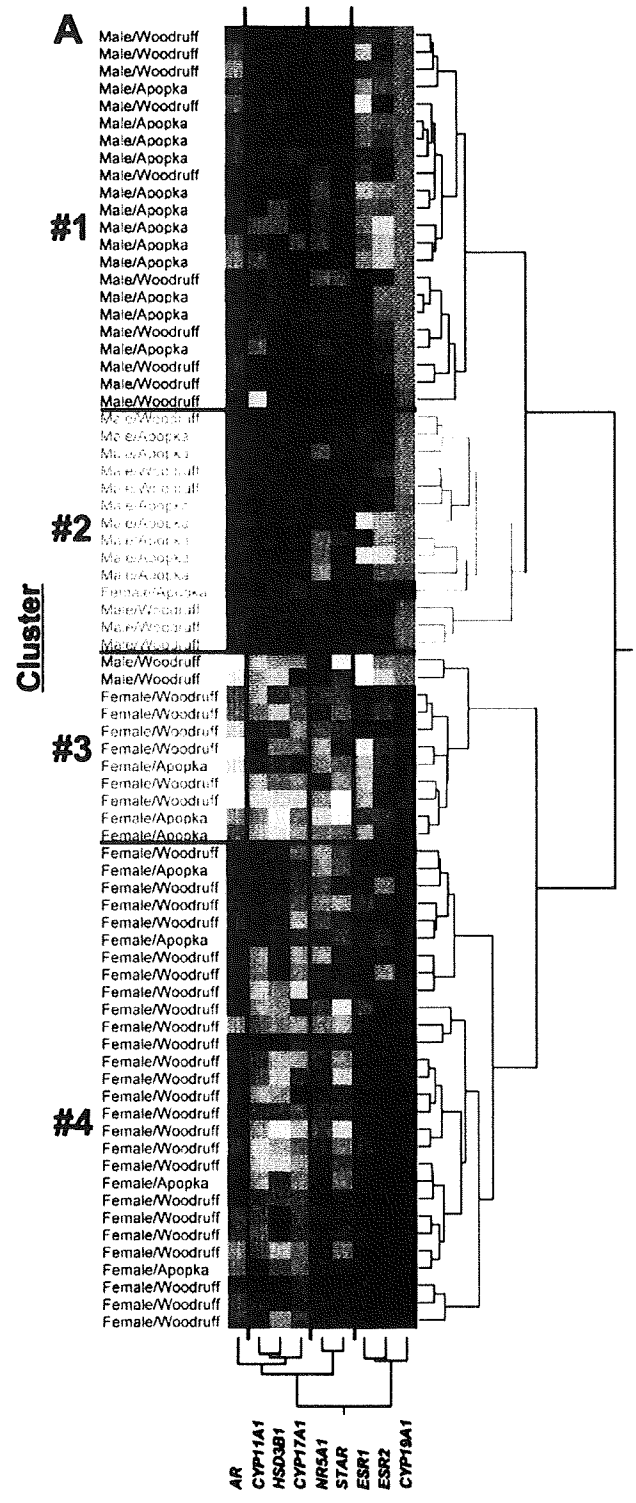

FIG. 5. Hierarchical cluster analysis of mRNA expression data from gonads of 13-mo-old Lake Woodruff and Lake Apopka alligators incubated at 32°C using Ward linkage clustering. The gray-scale, colorimetric gradient matrix displays lower expressions in lighter colors and higher expressions in darker colors. Dendrograms show distance scales for individual animals in the horizontal and mRNA expressions in the vertical. Sex and lake of origin of individual animals are noted to the left of the matrix. Horizontal lines separate numbered clusters. Vertical lines separate groups of similar gene expressions.

TABLE 3. Tukey-Kramer HSD post-hoc analysis of mRNA expressions from gonads of alligators from Lakes Woodruff and Apopka, incubated at 32°C; sex, number of animals, and lake of origin are also shown.

	mRNA transcript†									Sex			
										Male		Female	
Cluster no.*	*AR*[a]	*CYP11A1*[a]	*HSD3B1*[a]	*CYP17A1*[a]	*N45A1*[a]	*STAR*[a]	*ESR1*[a]	*ESR2*[a]	*CYP19A1*[a]	Woodruff	Apopka	Woodruff	Apopka
1	B	B	B	B	B	B	B,C	B	C	10	12	-	-
2	A	A	A	A	A	A	B	B	C	6	7	-	1
3	C	C	C	C	B	C	C	B	B	2	-	6	3
4	A	C	C	C	B	B,C	A	A	A	-	-	24	4

* Derived from hierarchical cluster analysis (Fig. 5).
† Uppercase letters represent differing Tukey-Kramer HSD post-hoc levels between clusters within each mRNA transcript.
[a] ANOVA $P < 0.001$.

sion that is orders of magnitude greater than testis expression [23, 24]. In light of this, our finding of a correlation between *AR* (but not *ESR1* or *ESR2*) and sexually dimorphic *CYP19A1* mRNA expression in the ovaries incubated at 32°C is notable.

In mammals, the roles of both estrogens and androgens in maintaining gonadal health, regardless of sex, is becoming more apparent. In neonatal mouse testes, inactivation of ESR2 increases the number of gonocytes and testosterone production, whereas an inactivation of ESR1 hypertrophies Leydig cells and increases the expression of steroidogenic enzymes [25]. In contrast, neonatal estradiol benzoate treatment of rats alters testicular steroid receptor expression during subsequent postnatal/peripubital development, in which mRNA expressions of *Esr1* and *Ar* decrease and that of *Esr2* increases [26]. Recent reviews highlight a growing understanding of the role androgen receptor activity plays in enhancing mammalian ovarian follicle development [27, 28]. Female mice that are deficient in androgen receptor are subfertile, have impaired folliculogenesis, show accelerated follicle depletion similar to premature ovarian failure, and exhibit reduced levels of specific growth factors [27–29]. Conversely, appropriate estrogenic signaling is vital to the establishment and maintenance of testis health [25, 30–32]. Adult *Esr1* knockout mice have impaired spermatogenesis, which is marked by decreased numbers of developing germ cells, decreased testis weights, larger Leydig cells, and increased levels of both circulating and testicular testosterone [33]. Additionally, testes of ESR2 knockout adult mice have increased numbers of smaller Leydig cells and increased numbers of spermatagonia per testis. In summary, this research supports the idea that in bird and mammals, both estrogen and androgen signaling play necessary roles in ovary and testis alike, and it demonstrates that extreme sexual dimorphic steroid receptor expressions in juvenile alligator gonads should not be expected.

If levels of steroid receptors are not expressed in highly sexually dimorphic manners but other steroidogenic enzymes, such as *CYP19A1* and *CYP11A1*, show more pronounced sexually dimorphic expressions, what associations can be found both within and between sex steroid receptor and steroidogenic factor and enzyme expressions? Cluster analysis revealed that these expression patterns are more complex than can be explained simply by sex or environment. In cluster analyses of mRNA expression data from both experimental groups. almost all males and females segregated at the earliest stages of hierarchical clustering. Subsequently, males and females segregated into primarily same-sex clusters of similar gene expression patterns. Analysis of mRNA expression levels across these clusters showed that only *CYP19A1* expression is uniformly sexually dimorphic. In comparison, the steroidogenic factors, enzymes, and sex steroid receptors investigated here showed expression patterns that, when compared between clusters, range from partial sexual dimorphisms to no correlation between sex and gene expression. Expressions of steroidogenic enzymes *HSD3B1*, *CYP11A1*, and *CYP17A1* were greater in all the male clusters of the 32°C incubation cohort (Fig. 5); however, expression levels of these enzymes in some the 33.5°C male clusters were equivalent to 30°C female expression levels (Fig. 4). The prosteroidogenic factors *NR5A1* and *STAR* showed the highest expression in some male clusters, but the expression levels in other male clusters of both incubation cohorts were equivalent to female expression levels. Therefore, elevated *CYP19A1* expression is a clear steroidogenic marker of ovary, whereas elevated *HSD3B1*, *CYP11A1*, and *CYP17A1* mRNA expression is indicative, but not diagnostic, of testis. Expression of the prosteroidogenic factors *NR5A1* and *STAR* is male-biased but displays substantial expression variability.

When examined across clusters, *ESR2* showed greater levels of sexual dimorphism and mRNA expression patterns more similar to those of *CYP19A1* expression than *ESR1* expression in both incubation temperature cohorts. A female cluster always showed the highest expression levels of *ESR1* or *ESR2*, however, *ESR1* and *ESR2* expression levels were equivalent between some predominantly male and female clusters. *AR* mRNA expression patterns grouped with *CYP19A1* in the 30 or 33.5°C cohort, but more closely with *HSD3B1*, *CYP11A1*, and *CYP17A1* in the 32°C cohort. Furthermore, *AR* mRNA expression did not display sexually dimorphic expression between male and female clusters in either study design. Therefore, whereas estrogen receptor expressions trended toward higher expression in ovaries, *AR* mRNA expression showed greater intrasex than intersex variability.

In the present study, we demonstrated that both ovary and testis show a similar relative mRNA expression pattern of steroid receptors, in which *ESR1* > *AR* > *ESR2*. However, both sex and environment can modulate expression patterns. Elevated *CYP19A1* and *ESR2* mRNA expressions are more diagnostic of alligator ovary, whereas elevated *HSD3B1*, *CYP11A1*, and *CYP17A1* mRNA expressions are most indicative of alligator testis. Other gonadal mRNA expressions, such as those of *AR*, *ESR1*, and *NR5A1*, show variable expression patterns that are not entirely associated with sex.

ACKNOWLEDGMENTS

The present study was possible through the continuing logistical support of our alligator research by the Florida Fish and Wildlife Conservation Commission; specifically, we thank Allan Woodward for his continued assistance with fieldwork and permitting. We also thank Elizabeth Swiman and Teresa Bryan for providing animal care.

REFERENCES

1. Iguchi T, Katsu Y. Commonality in signaling of endocrine disruption from snail to human. Bioscience 2008; 58:1061–1067.
2. Milnes MR, Bryan TA, Katsu Y, Kohno S, Moore BC, Iguchi T, Guillette LJ. Increased posthatching mortality and loss of sexually dimorphic gene expression in alligators (*Alligator mississippiensis*) from a contaminated environment. Biol Reprod 2008; 78:932–938.
3. Kohno S, Bermudez DS, Katsu Y, Iguchi T, Guillette LJ. Gene expression patterns in juvenile American alligators (*Alligator mississippiensis*) exposed to environmental contaminants. Aquat Toxicol 2008; 88:95–101.
4. Guillette LJ, Crain DA, Gunderson MP, Kools SAE, Milnes MR, Orlando EF, Rooney AA, Woodward AR. Alligators and endocrine disrupting contaminants: a current perspective. Am Zool 2000; 40:438–452.
5. Guillette LJ, Gunderson MP. Alterations in development of reproductive and endocrine systems of wildlife populations exposed to endocrine-disrupting contaminants. Reproduction 2001; 122:857–864.
6. Milnes MR, Bermudez DS, Bryan TA, Gunderson MP, Guillette LJ. Altered neonatal development and endocrine function in *Alligator mississippiensis* associated with a contaminated environment. Biol Reprod 2005; 73:1004–1010.
7. Fujisaki I, Rice KG, Woodward AR, Percival HF. Possible generational effects of habitat degradation on alligator reproduction. J Wildl Manage 2007; 71:2284–2289.
8. Guillette LJ, Brock JW, Rooney AA, Woodward AR. Serum concentrations of various environmental contaminants and their relationship to sex steroid concentrations and phallus size in juvenile American alligators. Arch Environ Contam Toxicol 1999; 36:447–455.
9. Heinz GH, Percival HF, Jennings ML. Contaminants in American alligator eggs from Lake Apopka, Lake Griffin, and Lake Okeechobee, Florida. Environ Monit Assess 1991; 16:277–285.
10. Ferguson MWJ, Joanen T. Temperature-dependent sex determination in *Alligator mississippiensis*. J Zool 1983; 200:143–177.
11. Hand DJ, Heard NA. Finding groups in gene expression data. J Biomed Biotechnol 2005; 2:215–225.
12. Milnes MR, Allen D, Bryan TA, Sedacca CD, Guillette LJ. Developmental effects of embryonic exposure to toxaphene in the American alligator (*Alligator mississippiensis*). Comp Biochem Physiol C Toxicol Pharmacol 2004; 138:81–87.
13. Ferguson MW. Reproductive biology and embryology of the crocodilians. In: Gleason PJ (ed.), Biology of the Reptilia, vol. 14. New York: John Wiley and Sons; 1985:329–491.
14. Gunderson MP, Kohno S, Blumberg B, Iguchi T, Guillette LJ. Up-regulation of the alligator CYP3A77 gene by toxaphene and dexamethasone and its short term effect on plasma testosterone concentrations. Aquat Toxicol 2006; 78:272–283.
15. Katsu Y, Bermudez DS, Braun EL, Helbing C, Miyagawa S, Gunderson MP, Kohno S, Bryan TA, Guillette LJ, Iguchi T. Molecular cloning of the estrogen and progesterone receptors of the American alligator. Gen Comp Endocrinol 2004; 136:122–133.
16. Valleley EMA, Harrison CJ, Cook Y, Ferguson MWJ, Sharpe PT. The karyotype of *Alligator mississippiensis*, and chromosomal mapping of the zfy/x homolog, zfc. Chromosoma 1994; 103:502–507.
17. Nakamura T, Katsu Y, Watanabe H, Iguchi T. Estrogen receptor subtypes selectively mediate female mouse reproductive abnormalities induced by neonatal exposure to estrogenic chemicals. Toxicology 2008; 253:117–124.
18. Ramsey M, Crews D. Steroid signaling system responds differently to temperature and hormone manipulation in the red-eared slider turtle (*Trachemys scripta elegans*), a reptile with temperature-dependent sex determination. Sex Dev 2007; 1:181–196.
19. Rhen T, Metzger K, Schroeder A, Woodward R. Expression of putative sex-determining genes during the thermosensitive period of gonad development in the snapping turtle, *Chelydra serpentina*. Sex Dev 2007; 1:255–270.
20. Yoshimura Y, Chang C, Okamoto T, Tamura T. Immunolocalization of androgen receptor in the small, preovulatory, and postovulatory follicles of laying hens. Gen Comp Endocrinol 1993; 91:81–89.
21. Dornas RAP, Oliveira AG, Dias MO, Mahecha GAB, Oliveira CA. Comparative expression of androgen receptor in the testis and epididymal region of roosters (*Gallus domesticus*) and drakes (*Anas platyrhynchos*). Gen Comp Endocrinol 2008; 155:773–779.
22. Katoh H, Ogino Y, Yamada G. Cloning and expression analysis of androgen receptor gene in chicken embryogenesis. FEBS Lett 2006; 580: 1607–1615.
23. Koba N, Mori M, Ha Y, Mizushima S, Tsukada A, Saito N, Ono T, Shimada K. Effects of aromatase inhibitor (fadrozole)-induced sex reversal on gonadal differentiation and mRNA expression of p450arom, AMH and ER alpha in embryos and growth in posthatching quail. J Poultry Sci 2008; 45:116–124.
24. Koba N, Ohfuji T, Ha Y, Mizushima S, Tsukada A, Saito N, Shimada K. Expression of p450arom, AMH and ER alpha mRNA in gonads of turkey, duck and goose within one week of age. J Poultry Sci 2008; 45:220–226.
25. Delbes G, Levacher C, Habert R. Estrogen effects on fetal and neonatal testicular development. Reproduction 2006; 132:527–538.
26. Tena-Sempere M, Navarro J, Pinilla L, Gonzalez LC, Huhtaniemi I, Aguilar E. Neonatal exposure to estrogen differentially alters estrogen receptor alpha and beta mRNA expression in rat testis during postnatal development. J Endocrinol 2000; 165:345–357.
27. Walters KA, Allan CM, Handelsman DJ. Androgen actions and the ovary. Biol Reprod 2008; 78:380–389.
28. Matsumoto T, Shiina H, Kawano H, Sato T, Kato S. Androgen receptor functions in male and female physiology. J Steroid Biochem Mol Biol 2008; 109:236–241.
29. Shiina H, Matsumoto T, Sato T, Igarashi K, Miyamoto J, Takemasa S, Sakari M, Takada I, Nakamura T, Metzger D, Chambon P, Kanno J, et al. Premature ovarian failure in androgen receptor-deficient mice. Proc Natl Acad Sci U S A 2006; 103:224–229.
30. O'Donnell L, Robertson KM, Jones ME, Simpson ER. Estrogen and spermatogenesis. Endocr Rev 2001; 22:289–318.
31. Sierens JE, Sneddon SF, Collins F, Millar MR, Saunders PTK. Estrogens in testis biology. Ann NY Acad Sci 2005; 1061:65–76.
32. Akingbemi BT. Estrogen regulation of testicular function. Reprod Biol Endocrinol 2005; 3:51.
33. Gould ML, Hurst PR, Nicholson HD. The effects of estrogen receptors alpha and beta on testicular cell number and steroidogenesis in mice. Reproduction 2007; 134:271–279.